Calibration of the CMS drift tube chambers and measurement of the drift velocity with cosmic rays

PUBLISHED BY IOP PUBLISHING FOR SISSA

RECEIVED: *November 26, 2009*
REVISED: *January 14, 2010*
ACCEPTED: *January 26, 2010*
PUBLISHED: *March 19, 2010*

COMMISSIONING OF THE CMS EXPERIMENT WITH COSMIC RAYS

Calibration of the CMS drift tube chambers and measurement of the drift velocity with cosmic rays

CMS Collaboration

ABSTRACT: This paper describes the calibration procedure for the drift tubes of the CMS barrel muon system and reports the main results obtained with data collected during a high statistics cosmic ray data-taking period. The main goal of the calibration is to determine, for each drift cell, the minimum time delay for signals relative to the trigger, accounting for the drift velocity within the cell. The accuracy of the calibration procedure is influenced by the random arrival time of the cosmic muons relative to the LHC clock cycle. A more refined analysis of the drift velocity was performed during the offline reconstruction phase, which takes into account this feature of cosmic ray events.

KEYWORDS: Large detector systems for particle and astroparticle physics; Particle tracking detectors (Gaseous detectors)

ARXIV EPRINT: 0911.4895

doi:10.1088/1748-0221/5/03/T03016

2010 JINST 5 T03016

Contents

2010 JINST 5 T03016

1 Introduction

The Compact Muon Solenoid (CMS) [1] is a general-purpose detector whose main goal is to explore physics at the TeV scale, by exploiting the proton-proton collisions provided by the Large Hadron Collider (LHC) [2] at CERN.

CMS uses a right-handed coordinate system, with the origin at the nominal collision point, the x-axis pointing to the center of the LHC, the y-axis pointing up (perpendicular to the LHC plane), and the z-axis along the anticlockwise-beam direction. The polar angle, θ, is measured from the positive z-axis and the azimuthal angle, ϕ, is measured in the x-y plane.

The central feature of the Compact Muon Solenoid apparatus is a superconducting solenoid, of 6 m internal diameter, providing a field of 3.8 T. Within the field volume are the silicon pixel and strip tracker, the crystal electromagnetic calorimeter (ECAL) and the brass/scintillator hadron calorimeter (HCAL). Muons are measured in gas-ionization detectors embedded in the steel return yoke. In addition to the barrel and endcap detectors, CMS has extensive forward calorimetry.

The barrel muon system [3] is divided in five wheels. Every wheel is composed of 12 sectors, each covering 30° in azimuth, as shown in figure 1.

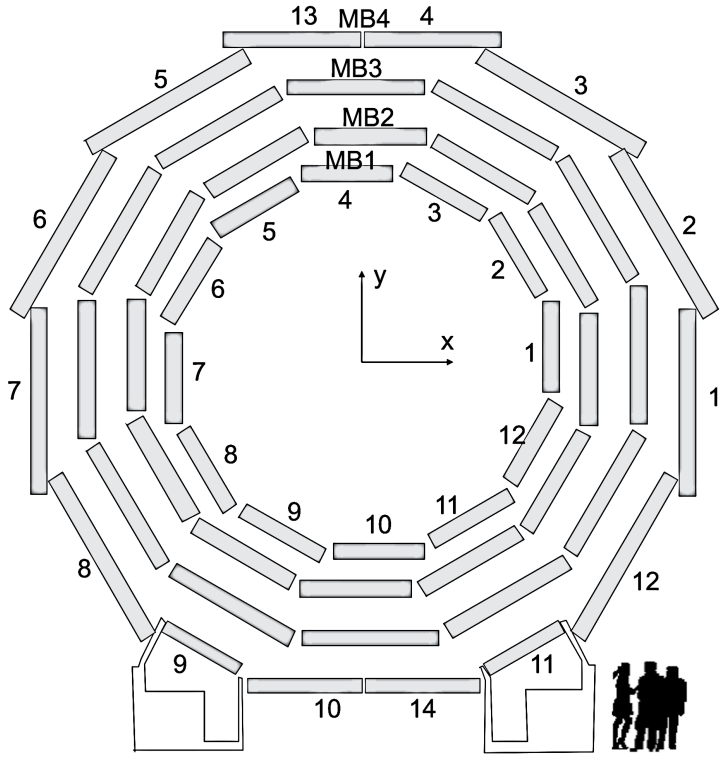

Figure 1. Schematic representation, in the $x-y$ plane, of the chamber positions within a wheel of the muon barrel system of the CMS experiment. The labels and the numbers of the muon stations are shown. Because of mechanical requirements, the top and bottom MB4 sectors are split in two distinct chambers.

Each sector contains four stations equipped with Resistive Plate Chambers (RPC) and Drift-Tubes (DT) chambers. The four DT chambers are labeled MB1, MB2, MB3, and MB4 going inside-out. In total there are 5 wheels $*$ (3 stations $*$ 12 sectors $+$ 1 station $*$ 14 sectors) $=$ 250 DT chambers. The chambers are interleaved with the steel return yoke of the magnet and are composed of three groups, called "super-layers" (SL), of four staggered layers of independent drift cells, for a total of about 172 000 channels. A schematic representation of a chamber is shown in figure 2 (left).

The chamber volume is filled with a Ar(85 %)/CO_2(15 %) gas mixture, kept at atmospheric pressure. Two of the super-layers have the wires parallel to the beam direction and measure the $r\phi$ coordinate, the other super-layer has wires perpendicular to the beam direction and measures the z coordinate. The chamber provides a measurement of a track segment in space. The outermost station is equipped with chambers containing only the two $r\phi$ super-layers. The basic element of the DT detector is the drift cell, illustrated in figure 2 (right), where the drift lines and isochrones are represented. All chambers were operational, fully commissioned, and the number of problematic channels were less than 1 %.

The DT system is designed to provide muon track reconstruction, with the correct charge assignment up to TeV energies, and first-level trigger selection. It also yields a fast muon identification and an accurate online transverse momentum measurement, in addition to single bunch-crossing identification with good time resolution. The good mechanical precision of the chambers allows the track segments to be reconstructed with a resolution better than 250 μm [3].

2010 JINST 5 T03016

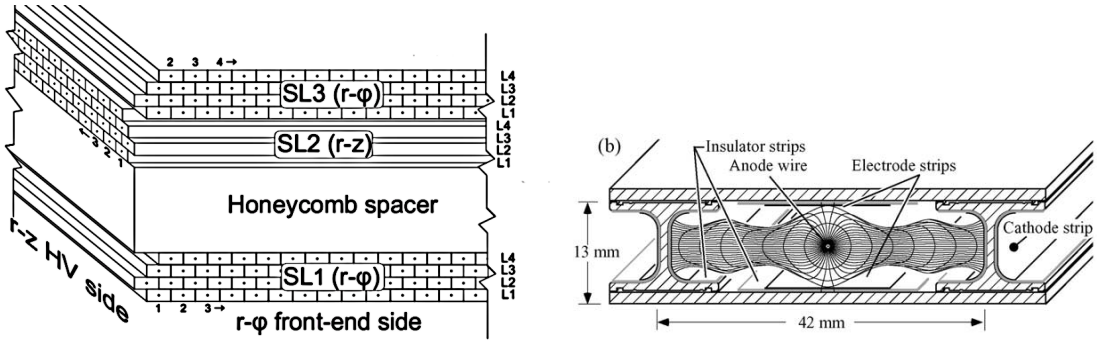

Figure 2. Left: Schematic view of a DT chamber. Right: section of a drift tube cell showing drift lines and isochrones. The voltages applied are +3600 V for wires, +1800 V for electrode strips, and −1200 V for cathode strips.

A fundamental ingredient of the DT system is the calibration, which is used as input to the local hit reconstruction, within the drift cells, and thereby influences the precision of the track reconstruction. This paper describes in detail the DT calibration procedures, to obtain reliable calibration constants, and presents results obtained from the extensive commissioning run with cosmic ray events performed in Autumn 2008, the Cosmic Run At Four Tesla (CRAFT) [4], in preparation for LHC running.

The data sample used for the calibration process and the trigger conditions are summarized in section 2. The main characteristics of the DT calibration process are described in section 3. The process consists in the determination of the inter-channel synchronization, described in section 4, the analysis of noisy channels, treated in section 5, and the calculation of the time pedestals and the drift velocity, described in sections 6 and 7, respectively. The DT calibration workflow, including the monitoring of the conditions, is performed within the CMS computing framework, as described in section 8. Finally, a more refined analysis of the drift velocity in the muon system, within the offline reconstruction process, is presented in section 9.

2 Cosmic ray event trigger and the data sample

The long cosmic ray data taking in 2008 with and without magnetic field allowed a detailed study of the DT drift properties and an improved understanding of the calibration constants. About 270 million events were collected with a 3.8 T field inside the solenoid magnet. In this configuration, the radial component of the magnetic field in the DT chamber positions does not exceed 0.8 T.

The DT system was the primary trigger source for most of the collected events. The local trigger [3] was designed to operate with collisions taking place at the center of the CMS detector, and it is performed searching the ϕ-matching of hits in each chamber. This is achieved using dedicated hardware, which configures the expected track paths from one chamber to another.

Due to the different origin, direction, and timing of the cosmic rays, as compared to muons from proton-proton collisions, dedicated adjustments were needed to properly configure the DT trigger for high efficiency during CRAFT. This required relaxing the extrapolation algorithm with a particular configuration of the DTTF (DT Track Finder) as explained in more detail in ref. [5].

2010 JINST 5 T03016

Therefore, during data-taking with cosmic rays, the L1 trigger was generated by the coincidence in time of two segments in two stations of the same sector, or adjacent sectors, and a rate of about 240 Hz was provided to the Global Muon Trigger.

About 20 million events, out of the 270 million collected during CRAFT, were used for the calculation of the calibration constants. They have been chosen from stable runs where most of the DT system was operational. No quality cuts are, in principle, necessary to perform the calibration. However, in order to have a clean sample of muons, a transverse momentum cut of 7 GeV was applied.

3 The calibration process

Charged particles crossing a DT cell produce ionization electrons in the gas volume. The determination of the relationship between the arrival time of the ionization signal and its spatial deposition is the primary goal of the calibration task, which leads to the extraction of the drift times and drift velocities.

The arrival time of the ionization signal is measured using a high performance Time to Digital Converter (TDC) [6]. This is the main building block of the read-out boards of the DT system. It is a multi-hit device in which all hits within a programmable time window, large enough to accommodate the cell maximum drift time, are assigned to each Level 1 Accept trigger. The drift time is directly obtained from the time measured by the TDC, after subtracting a time pedestal which contains contributions from the latency of the trigger and the propagation time of the signal, within the detector and the data acquisition chain. The first goal of the calibration procedure is, therefore, to determine the time pedestals, as described in section 6. The expected precision of the time pedestal calibration during the cosmic ray data-taking is limited by the arrival time distribution of cosmic rays which is flat within the clock cycle and it is of the order of $25\ \mathrm{ns}/\sqrt{12}$.

The other relevant quantity for the DT calibration process is the effective drift velocity. It depends on many parameters, including the gas purity and the electrostatic configuration of the cell, the presence of a magnetic field within the chamber volume, and the inclination of the track. The parameters connected to the working conditions of the chambers are monitored continuously [3]: the high voltage supplies have a built-in monitor for each channel; the gas is at room temperature and its temperature is measured on each preamplifier board inside the chamber; the gas pressure is regulated and measured at the gas distribution rack on each wheel, and is monitored by four further sensors placed at the inlet and outlet of each chamber. The adequacy of the flow sharing from a single gas distribution rack to 50 chambers is monitored at the inlet and outlet line of each individual chamber. A possible leakage in the gas line can be sensed via the flow and/or the pressure measurements.

Five small gas chambers, one for each wheel, are used to measure the drift velocity in a volume of very homogeneous electric field, located in the accessible gas room adjacent to the cavern, outside of the CMS magnetic field. Each of these chambers, called Velocity Drift Chambers (VDC) [7, 8], is able to selectively measure the gas being sent to, and returned from, each individual chamber of the wheel thus providing rapid feedback on any changes due to the gas mixture or contamination. During the CRAFT data-taking period only one such chamber was used.

2010 JINST 5 T03016

No noticeable variation of the parameters described above is expected among different regions of the spectrometer. However, the magnetic field and the track impact angle may vary substantially from chamber to chamber, as they occupy different positions in the return yoke.

Two methods for calculating the electron drift velocity in a DT cell are presented here. They both assume a constant drift velocity in a given chamber. The first method, discussed in section 7, is based on the measurement of the effective drift velocity using the mean-time technique, which computes the velocity value at the super-layer granularity level. The second method, discussed in section 9, relies on the muon track fit, which determines track-by-track the time of passage of the muon and the drift velocity as additional free parameters of the fit, together with the track position and inclination angle. The assumption of a constant drift velocity is considered a good approximation because the magnetic field in the chamber volume is usually low and approximately homogeneous. A third method based on a parameterization of the drift velocity as a function of the drift time, the magnetic field, and the muon trajectory is discussed in ref. [9].

The detailed drift velocity analysis, described in section 9, also reveals non-linear effects in the innermost stations (MB1 chambers) of the barrel external wheels (Wheel +2 and Wheel -2), where the strongest radial magnetic field component, of about 0.8 T, is present.

The DT calibration process also depends on the different signal path lengths to the read-out electronics (called inter-channel synchronization time) and on the list of noisy channels, as will be described in the following sections.

4 The inter-channel synchronization

The inter-channel synchronization is calculated for each read-out channel of each chamber, in order to correct for the different signal path lengths of trigger and read-out electronics. This is a fixed offset, since it only depends on cable/fiber lengths, and it does not need to be re-calibrated very often. Nevertheless, it is useful to frequently redo its calibration, to monitor the correct behavior of the front-end electronics. The inter-channel synchronization is determined by test-pulse calibration runs. The design of the data acquisition system allows such runs to be taken during the normal physics data-taking, by exploiting the collision-free interval of the LHC beam structure, called "abort gap".

During special calibration runs, a test-pulse is simultaneously injected in four channels of a front-end board, each one from a different layer of a super-layer, simulating a muon crossing the super-layer. To perform the scanning of the entire DT system in only 16 cycles, the same test-pulse signal is also distributed to other four-channel groups, 16 channels apart.

The so-called t_0 calibration consists in determining, for each DT channel, the mean time and the standard deviation of the test-pulse. In the calibration procedure, the events are split in two samples: the first is used to compute the average value, within a full chamber, of the signal propagation time from the test-pulse injector to the read-out electronics; the second is used to calculate, for each individual channel, the difference between the time of its test-pulse signal and the average value of the chamber.

Figure 3 shows an example of a distribution of t_0 constants for representative layers of the three super-layers of a chamber, as a function of the channel number. The other layers show very similar t_0 values. The t_0 synchronization correction is always below 10 ns (1 TDC count corresponds

2010 JINST 5 T03016

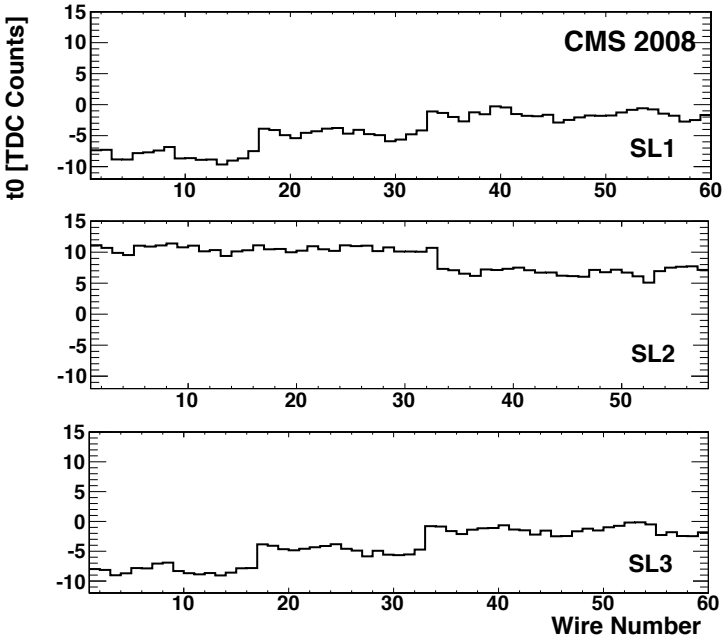

Figure 3. Inter-channel synchronization constants calculated from a test-pulse run. The results are shown for three representative layers, belonging to each of the three super-layers of chamber MB3 in Sector 9. The step-function shape reflects the grouping of channels among different front-end boards.

to 0.78 ns). The standard deviation is about 1 ns, for all channels. This is compatible with the precision of the electronic chain. These corrections correspond to the distance between the front-end boards, located inside the chamber volume, and the read-out boards. Wires connected to a given front-end board belong to cells adjacent to each other, in the super-layer, and have approximately the same distance up to the read-out boards. This leads to the step-function shape seen in figure 3, more pronounced in the super-layers 1 and 3.

5 Noise analysis in the DT chambers

On the basis of systematic studies performed during several commissioning phases of the DT detector, a cell is defined as noisy if its hit rate at operating voltage, counting signals higher than a common discriminator threshold of 30 mV, is higher than 500 Hz.

The number and geometrical distribution of noisy DT channels have been studied, in particular, during a commissioning period without magnetic field and having the detector wheels separated from each other. In this section we describe the results of the noise analysis performed using the cosmic ray events collected during CRAFT. With respect to runs using random triggers, the noise analysis based on normal data taking runs has the advantage of reflecting the detector operation in more realistic conditions.

The first aim of the noise studies is to check the stability of the number of noisy cells in different conditions of the CMS detector. For all runs analyzed, the number of noisy cells is around 0.01 % of all DT channels. The rate of noise hits per cell is shown in figure 4, for a number of representative runs, with and without magnetic field, and with different sub-detectors included in

2010 JINST 5 T03016

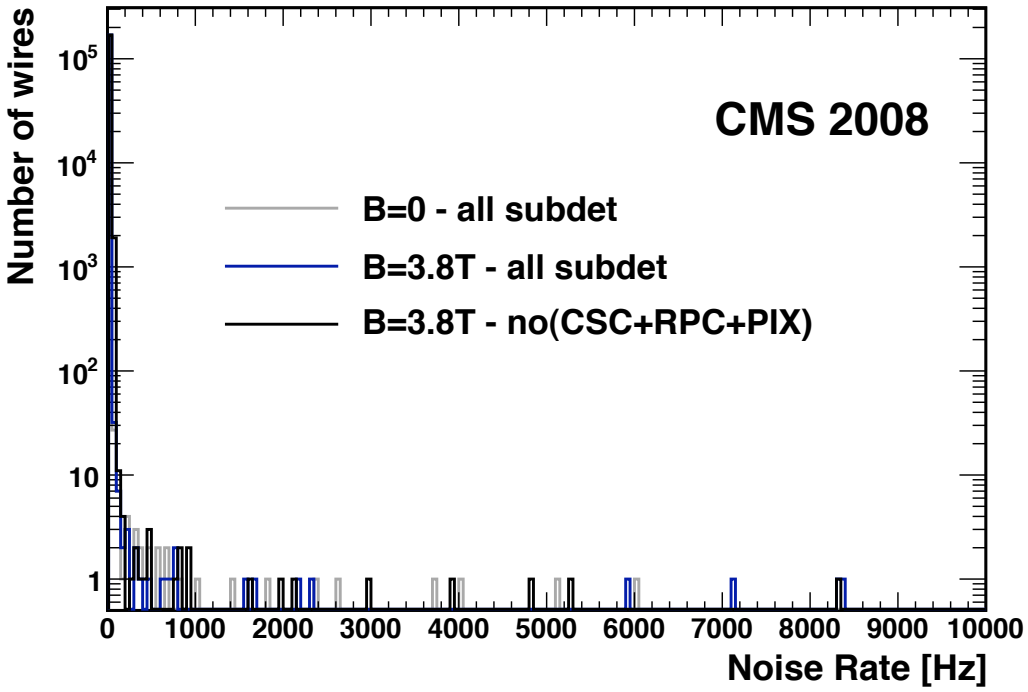

Figure 4. Distribution of the cell noise rate for different data-taking conditions: with and without magnetic field; with and without Cathode Strip Chambers (CSC), Resistive Plate Chambers (RPC), and Pixels (PIX).

Table 1. Number of Noisy Cells in each chamber type (MB1, MB2, MB3, MB4) and average noise rate for some representative runs of different data-taking conditions. The results from the CRUZET (Cosmic RUn at ZEro Tesla) commissioning period are also shown, for comparison.

Data Period	B Field [T]	Excluded Sub-Det.	Number Noisy Cells in MB1	Number Noisy Cells in MB2	Number Noisy Cells in MB3	Number Noisy Cells in MB4	Mean Noise Rate [Hz]
CRUZET	0	CSC, PIX	12	2	2	0	3.96
CRAFT	0		0	13	3	2	3.80
CRAFT	3.8		13	3	1	2	4.15
CRAFT	3.8	CSC	12	7	0	8	4.23
CRAFT	3.8	CSC, PIX, RPC	17	5	0	0	4.50

the acquisition. The number of cells with a hit rate higher than 500 Hz is very small. Detailed information on the noise rate observed for representative runs, with different configurations of CMS detectors included in the data acquisition, is shown in table 1.

An average noise rate of ~ 4 Hz is observed in the DT system, essentially insensitive to the magnetic field and to the status of nearby sub-detectors. In addition, it has been observed that around 50 % of the noisy cells remain noisy for long data-taking periods.

2010 JINST 5 T03016

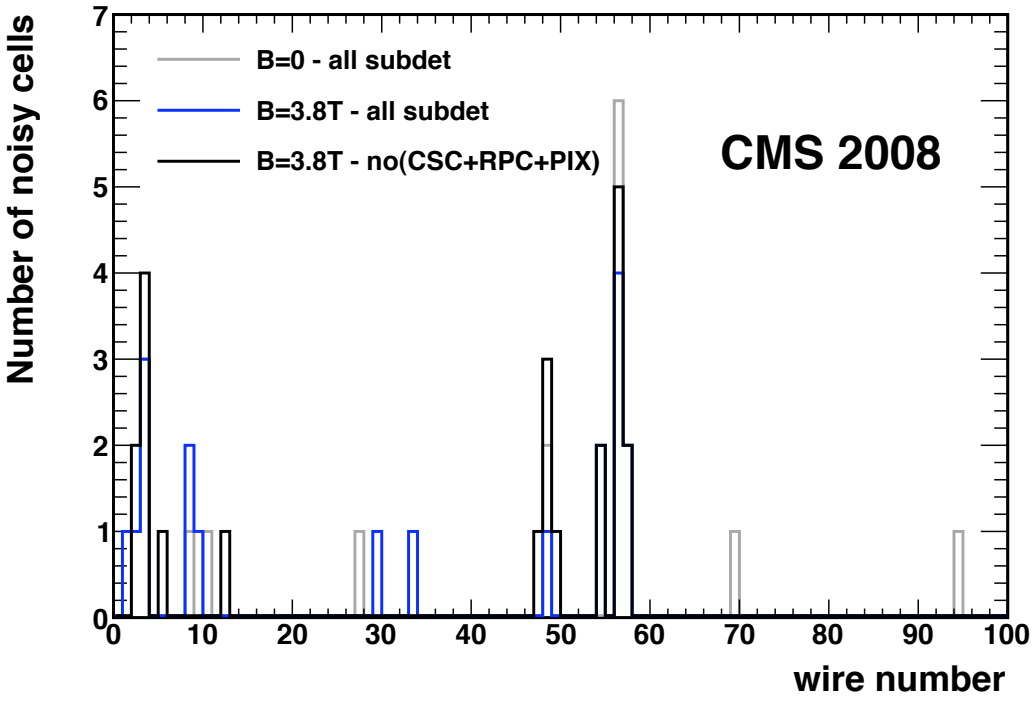

Figure 5. Number of noisy channels as a function of the wire number, for the data-taking periods mentioned in table 1. Each distribution corresponds to a different run and shows the noisy cells observed for chamber types MB1, MB2, MB3 and MB4.

Studies have also been made concerning the position dependence of the noisy cells, within wheels and chambers. As seen on table 1, most of the noisy channels are located in the innermost chambers (MB1), where the internal cabling is more complex, because of the reduced space. In figure 5, the noisy cell distribution is shown as a function of the wire number. The noisy cells appear concentrated in the regions of the super-layer close to the wire boundaries, which are different depending on the number of wires present in each chamber type (about 50 for MB1, 60 for MB2, 70 for MB3, and 90 for MB4). The peaks also reflect the position of the connectors distributing the HV inside the super-layer, which generate some electronic noise in their proximity.

The observed fraction of noisy cells (0.01 %) and the average noise rate (~ 4 Hz) in the full DT system are too low to affect the digitization efficiency or the trigger rate. It is important, however, to exclude the noisy cells in the calibration process described in the following sections.

6 The time pedestal calibration

6.1 Computation of the calibration constants

The time pedestal calibration is the process which allows the extraction of the drift time from the TDC measurement. For an ideal drift cell, the time distribution coming from the TDC (t_{TDC}) would coincide with the distribution of drift time (t_{drift}), and would have a box shape starting from a null drift time, for tracks passing near the anode, up to about 380 ns, for tracks passing near the cathode.

2010 JINST 5 T03016

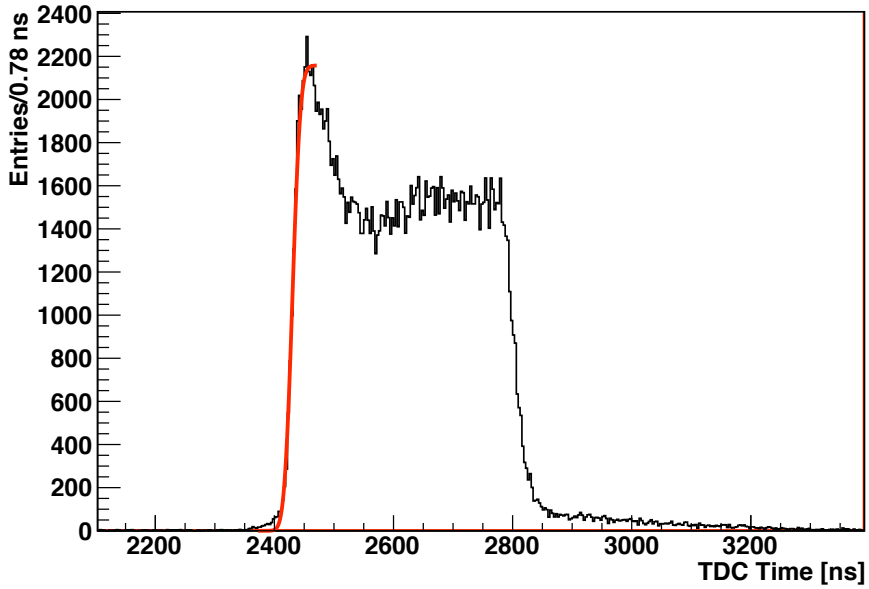

Figure 6. Distribution of the signal arrival times, recorded by the TDC, for all the cells of a single superlayer in a chamber, after the cell-to-cell equalization based on the test-pulse calibration. The continuous line indicates the fit of the *Time Box* rising edge to the integral of a Gaussian function.

Experimentally, some non-linear effects related to the electric field distribution inside the drift cell have to be considered in the response of these cells; they are enhanced by the track inclination and by the presence of the magnetic field. In addition, different time delays, related to trigger latency, and different cable lengths of the read-out electronics, also contribute to the TDC measurements. The time measured by the TDC, t_{TDC}, can be expressed as

$$t_{\mathrm{TDC}} = t_0 + t_{\mathrm{TOF}} + t_{\mathrm{prop}} + t_{\mathrm{L1}} + t_{\mathrm{drift}} \quad , \tag{6.1}$$

where

- t_0 is the inter-channel synchronization used to equalize the response of all the channels at the level of each chamber, as described in section 4;
- t_{TOF} is the Time-Of-Flight (TOF) of the muon, from the interaction point to the cell, in the case of collision events. In the case of cosmic events, this quantity cannot be defined because the time pedestal is an average of the arrival time of cosmic muons relative to the clock cycle;
- t_{prop} is the propagation time of the signal along the anode wire;
- t_{L1} is the latency of the Level-1 trigger;
- t_{drift} is the drift time of the electrons from the ionization cluster to the anode wire within the cell.

The main goal of the calibration is the calculation of the time pedestal, t_{trig}, which is dominated by the time delay caused by the L1 trigger latency:

$$t_{\mathrm{trig}} = t_{\mathrm{TOF}} + t_{\mathrm{prop}} + t_{\mathrm{L1}} \quad . \tag{6.2}$$

The value of $t_{\rm trig}$ is extracted for each super-layer directly from the $t_{\rm TDC}$ distribution, referred to as *Time Box*, after subtracting the noisy channels and correcting for the inter-channel synchronization. Figure 6 shows a *Time Box* measured during a CRAFT run, for one super-layer.

The value of $t_{\rm trig}$ is the turn-on point of the *Time Box* distribution. It is computed by fitting the rising edge of the distribution to the integral of a Gaussian function, as illustrated by the continuous line in figure 6. The procedure is applied at the super-layer level and is described in more detail in ref. [10].

The main quantities calculated by the fit are the inflexion point of the rising edge, $T_{\rm mean}$, and its standard deviation, $T_{\rm sigma}$, which represents the resolution of the measurement. Figure 7 shows the distributions of $T_{\rm mean}$ and $T_{\rm sigma}$ measured, in a CRAFT run with $B = 3.8$ T, for the innermost $r\phi$ super-layer of a representative wheel, as a function of chamber type and sector. Similar results were obtained for the other wheels. Approximately constant values are observed for chambers of the same type and for all the wheels. The periodic structure seen in the $T_{\rm mean}$ distribution, figure 7 (top), reflects the time-of-flight of the cosmic muon from the upper sector to the lower sector. Indeed, the events contributing to the calculation of $T_{\rm mean}$ and $T_{\rm sigma}$ can be triggered by the upper or lower sectors. The events triggered by the top (bottom) sectors may also be detected by other non-triggering sectors, having a less precise time pedestal and, consequently, leading to a less precise determination of these quantities. Different runs during the entire CRAFT period have been analyzed, and a stable performance of the whole DT system has been observed. As expected, no dependence on the magnetic field strength was observed.

The time resolution distribution, figure 7 (bottom), indicates the precision which the calibration procedure can reach with cosmic rays. A standard deviation of ~ 10 ns is observed for all super-layers in all wheels, except in the vertical sectors, where the number of events is limited and the muon crossing angles are large. The time resolution precision is limited mainly by the random arrival time of cosmic muons relative to the clock cycle. Furthermore, the resolution in Sector 1 is systematically worse than in Sector 7 because the trigger cables that distribute the Level 1 accept signal are longer and, therefore, generate larger skews in the signal transmission.

After the determination of $T_{\rm mean}$ and $T_{\rm sigma}$, the time pedestal, $t_{\rm trig}$, is estimated as

$$t_{\rm trig} = T_{\rm mean} - k \cdot T_{\rm sigma} \quad . \tag{6.3}$$

The k factor is evaluated by minimizing the position residuals, using the local reconstruction of track segments within chambers. After a few iterations, a k factor of 0.7 was computed for the CRAFT data and was applied to all super-layers. The position residuals were then recalculated and a final correction to the time pedestals was computed dividing the remaining offsets observed in the residual distributions by a constant drift velocity (54.3 μm/ns). The final $t_{\rm trig}$ constants were stored in a database, as described in section 8.

6.2 Validation of the calibration constants

Once the $t_{\rm trig}$ constants are computed, the calibration process proceeds with the validation step, which consists in studying the effect of these constants on the reconstruction algorithm. The analyzed quantities are the residuals computed, layer by layer, as the distance between the hit and the intersection of the 3D segment with the layer plane. A complete description of the local re-

2010 JINST 5 T03016

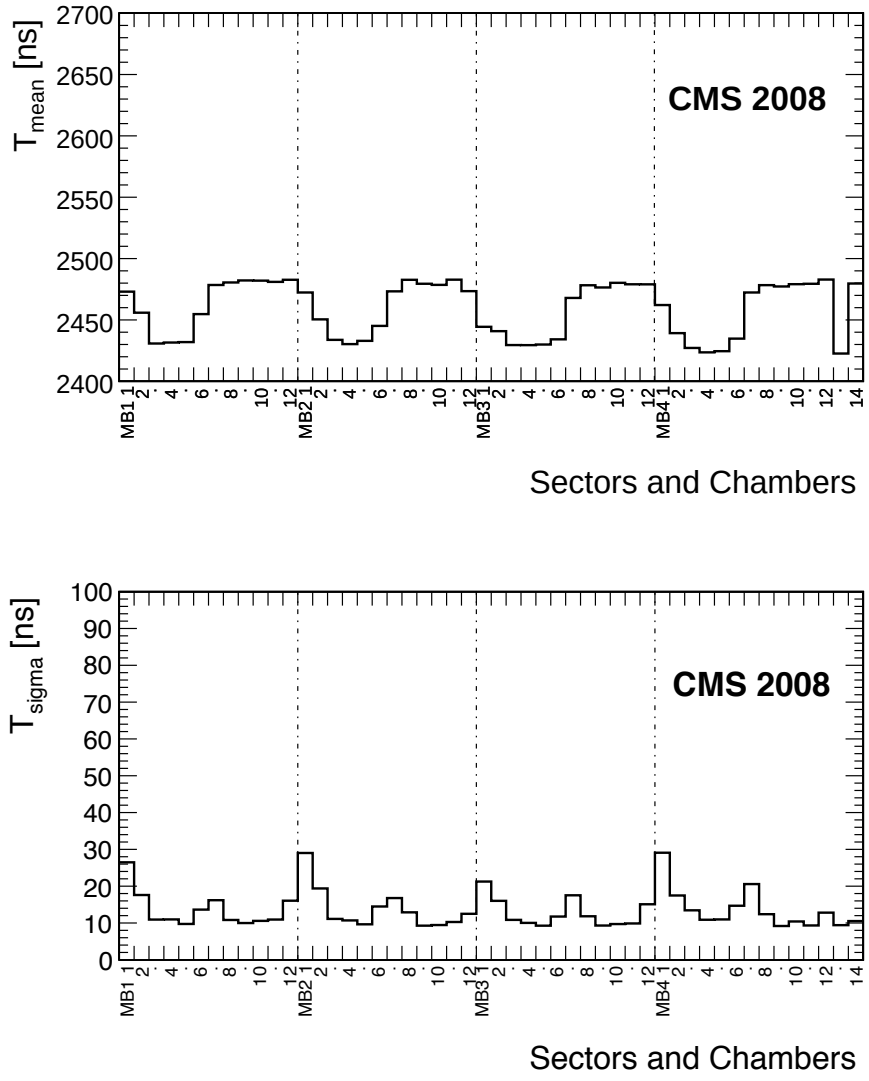

Figure 7. Mean (top) and standard deviation (bottom) of the fitted inflexion point of the *Time Box* rising edge, for the innermost $r\phi$ super-layer for a representative wheel. The triggering sectors (3, 4, 5 and 9, 10, 11) are synchronized among each other. The sectors with vertical chambers (sectors 1 and 7) detect much less cosmic ray muons, leading to a poorly defined rising edge and a less accurate calibration.

construction procedure is given in ref. [11]. To correct for the propagation time along the wire, the reconstruction of the segment is done in a multistep procedure. First the reconstruction is performed in the $r\phi$ and z projections independently. Once two projections are paired and the position of the segment inside the chamber is approximately known, the drift time is corrected for the propagation time along the wire and for the TOF within the super-layer, and the 3D position is updated.

The mean values of the residual distributions calculated for the innermost $r\phi$ super-layer for a representative wheel are shown in figure 8 (top). A systematic offset with respect to the origin is observed compatible with the systematic delay between the arrival time of the cosmic muon events

2010 JINST 5 T03016

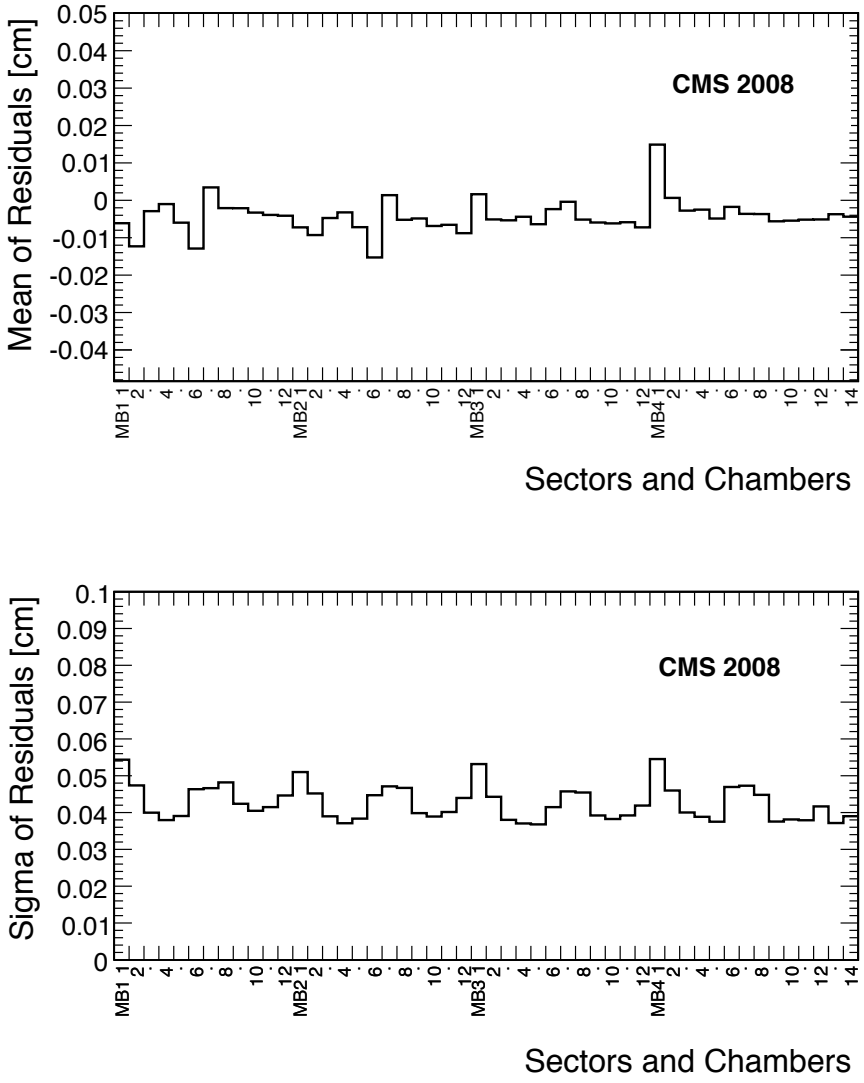

Figure 8. Mean (top) and width (bottom) Gaussian parameters, as fitted to the distributions of the residuals between the reconstructed hits and the reconstructed local segments. The results are shown for the $r\phi$ super-layers for a representative wheel, after correcting the offset with respect to the origin of the residual distribution. Other wheels show similar results.

and the clock cycle. The standard deviations of the fit to the residuals, shown in figure 8 (bottom) and in the range 400–600 μm, represent the spatial resolution obtained with the calibration process, a factor of two worse than the nominal resolution of about 250 μm [3]. The difference is caused by the spread of the muon arrival times inside the 25 ns time window associated with the L1 trigger. This dilution will not occur with LHC collision data.

2010 JINST 5 T03016

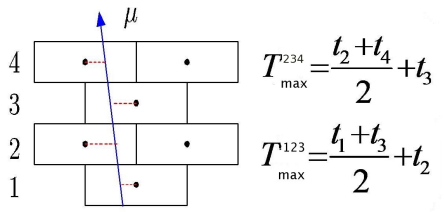

Figure 9. Schematic view of a super-layer section, showing the pattern of semi-cells crossed by a track. The quantities t_i in the equations represent the arrival time of the electrons within a drift cell.

7 The drift velocity calibration

The aim of the drift velocity calibration is to find the best effective drift velocity in each region of the DT system. In order to be consistent with the t_{trig} calculation, described in section 6, the drift-velocity calibration is computed with a super-layer granularity.

The calibration algorithm is based on the mean-time technique described in detail in ref. [10]. In this method, the maximum drift time in a cell, T_{max}, is calculated considering nearby cells in three adjacent layers and using a linear approximation to determine the average drift velocity. As an example, figure 9 shows the simplest pattern of a muon crossing a semi-column of cells, together with the equations used to calculate T_{max}. In general, T_{max} depends on the track inclination and on the pattern of cells crossed by the track. Taking into account these dependencies, a spread of about 28 ns has been observed in the calculation of T_{max} from CRAFT data.

The effective drift velocity can be estimated assuming a linear space-time relationship,

$$v^{\text{eff}}_{\text{drift}} = \frac{L_{\text{semi-cell}}}{< T_{\text{max}} >} \quad , \tag{7.1}$$

where $L_{\text{semi-cell}} = 2.1$ cm is half the width of a drift cell.

Drift velocities measured for each chamber/sector and for a representative wheel (other wheels give similar values) are shown in figure 10 for two CRAFT runs, one without (top) and one with (bottom) magnetic field. The drift velocity has approximately a constant value of 54.3 μm/ns, although with some systematic deviations, caused by limitations of the calibration procedure applied to cosmic ray events. As in the determination of the time pedestal, these uncertainties originate mainly from the random arrival time of cosmic muons relative to the clock cycle.

The t_{trig} uncertainty of about 10 ns, seen in figure 7 (bottom), corresponds to a relative uncertainty of about 2.5 % on the drift velocity. This is comparable to the fluctuations observed in figure 10, meaning that the residuals calculated with the $v^{\text{eff}}_{\text{drift}}$ and t_{trig} constants do not represent a significant improvement with respect to those shown in figure 8.

The drift velocity distribution measured in one of the VDC chambers (section 3) during the full CRAFT period is shown in figure 11. An average drift velocity value of 54.8 μm/ns is observed, which is slightly different (0.5 % higher) from the one obtained from the DT data, mainly because of the different shape of the electric field in the DT drift cell. The spread of the distribution is better than 0.2 μm/ns, and shows that no major variations occurred in the gas mixture or air contamination, during the entire data-taking period.

2010 JINST 5 T03016

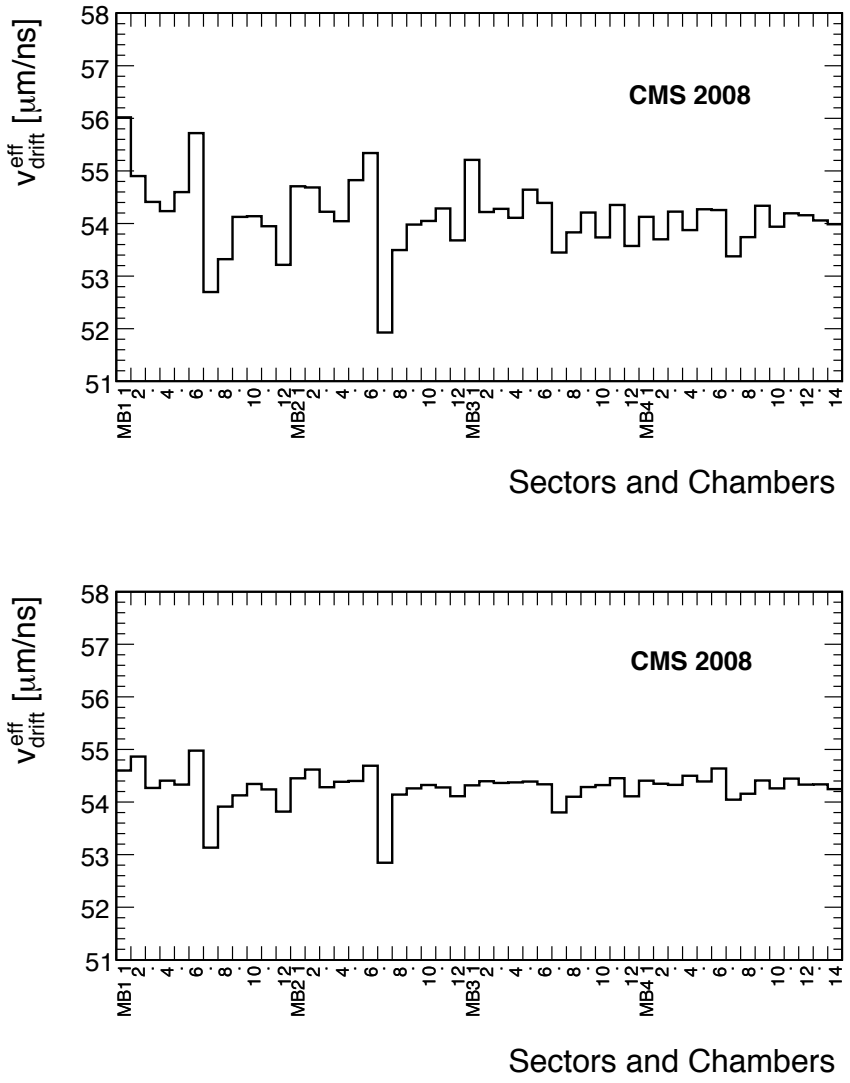

Figure 10. Drift velocities computed using the mean-time method for a run with $B = 0$ T (top) and for a run with $B = 3.8$ T (bottom). Results are shown for the $r\phi$ super-layers of each chamber/sector of a representative wheel. The other wheels show similar results.

8 The calibration workflow and the monitoring of the calibration process

A fast calibration of the DT system is vital in order to provide the prompt data reconstruction with accurate calibration constants. The number of calibration regions is a compromise between the need of keeping things simple, not requiring too large event samples, and the need of reducing systematic errors by separately calibrating regions where parameters may have very different values. As mentioned in previous sections, the super-layer granularity has been found to be the most suitable calibration unit.

In order to reach the precision obtainable with the fast calibration, about 10^4 tracks crossing

2010 JINST 5 T03016

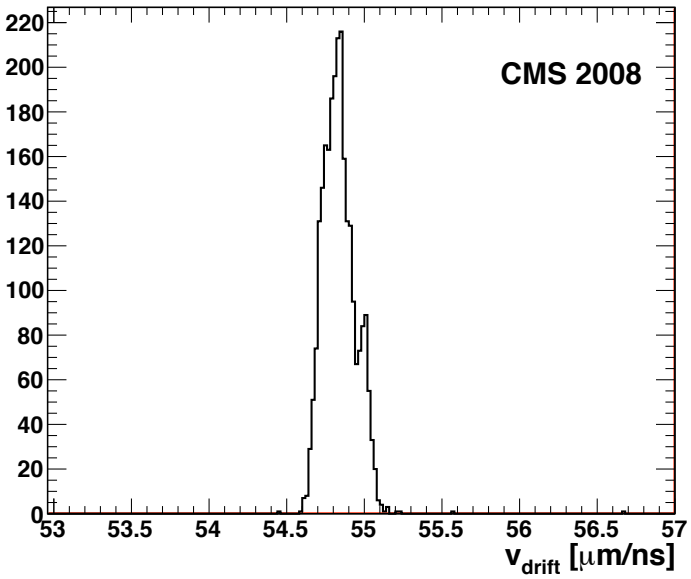

Figure 11. Distribution of the drift velocity measured in one Velocity Drift Chamber (VDC) during the entire data-taking period.

each super-layer are required. During LHC collision and cosmic ray data-taking periods, the calibration parameters have to be produced, validated, and made available for use in the reconstruction within one day of data-taking. However, after the start-up phase, it is anticipated that at some point it will no longer be necessary to update the DT calibrations on a daily basis; on the other hand, they should be checked against a standard set in order to guarantee their stability.

The workflow of the DT calibration has already been fully embedded into the central CMS calibration workflow at a very early stage. A more detailed description of the overall CMS calibration and alignment computing workflow used in the CRAFT exercise is given in refs. [12, 13]. Within the CMS calibration and alignment workflow, particular selections of data, named *AlCaReco*, were used. They contained a reduced number of events and a reduced event content, providing the minimal information to fulfill the requirements of the DT calibration task. The sample is saved at the CERN Analysis Facility (CAF) and taken as input to the calibration process. The calibration algorithm runs at the CAF and produces a set of constants, which undergoes a validation procedure before being copied to the central CMS database, where they become available to the CMSSW offline software framework.

The DT calibration workflow has been used also during the Computing, Software, and Analysis challenge (CSA08), described in ref. [12], which simulated with large event samples the conditions expected at LHC startup. This exercise simulated the production rate of the calibration conditions as it will happen during real collision data-taking. The long CRAFT data-taking period served as a thorough test of this workflow with the real detector.

The quality and stability of the calibration constants is a crucial part of the procedure and must be continuously monitored. Therefore, validation procedures have been set up within the central CMS Data Quality Monitoring (DQM) framework. A detailed description of the CMS DQM structure is given in ref. [14].

2010 JINST 5 T03016

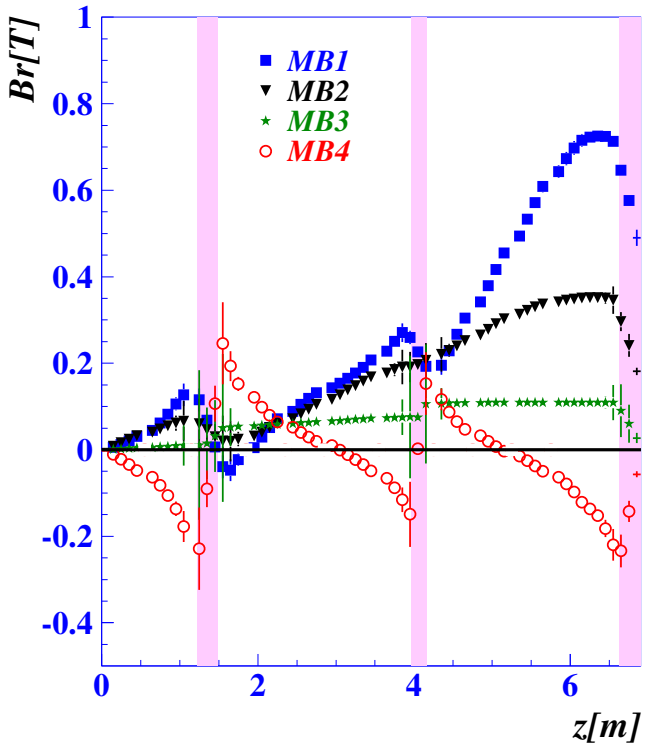

Figure 12. Computed radial component of the magnetic field in the muon barrel chambers, for the different wheels, as a function of z.

Data quality assessment for the DT calibration constants consists mainly in defining the acceptance criteria used to validate the constants, in the monitoring of time stability, and in the checking of continuous trends or sudden changes in operating conditions. The quality tests to assess the validation of the constants and to monitor their time stability are applied to the residual distributions calculated at the different steps of the calibration workflow. The comparison of the currently produced calibration constants with a reference set gives an indication of the stability of each particular calibration constant.

All the calibration constants described in the present paper have their validation as well as monitoring process, and for each of them detailed and summary DQM plots are provided. The DT condition constants have been monitored through the entire CRAFT data-taking period and have shown generally a good stability in time.

9 Drift velocity analysis

The drift velocity obtained with the calibration procedure described in section 7 is derived from the measurements of the drift time and, as already mentioned, is limited by the uncertainty on the arrival time of the cosmic ray muons.

A more detailed analysis of the drift velocity is presented in this section, taking into account the precise 3D space-time relationship for the hit reconstruction. In particular, it considers the influence of the magnetic field as a function of the position along the wire.

2010 JINST 5 T03016

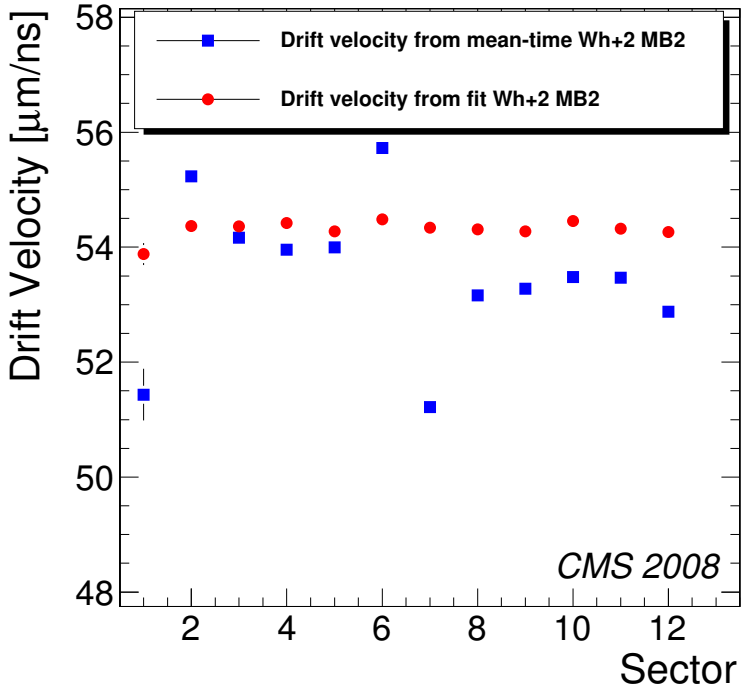

Figure 13. Mean values of the drift velocity for the MB2 chambers of Wheel +2, using the mean-time (squares) and fit (circles) methods. The differences between sectors when using the mean-time method are due to t_{trig} uncertainties that are not present in the fit method.

The presence of a radial magnetic field distorts the drift lines of the drifting electrons, because of the Lorentz force, resulting in a variation of the effective drift velocity. Figure 12 shows that the radial field component is not very high in the muon barrel chambers, except in the MB1 chambers of the outer wheels, closest to the endcaps. In these regions, the radial component of the magnetic field can be as high as 0.8 T, and changes significantly along the z axis, resulting in a variation of the effective drift velocity along the wire of each single cell, for $r\phi$ super-layers. The effect of the magnetic field has been studied in test beams with small prototypes [15], and more recently in the Magnet Test and Cosmic Challenge (MTCC), using cosmic rays in the CMS surface hall. These studies showed that the chambers maintain a good trigger and event reconstruction functionality, even in the most critical regions [16].

In the method presented in this section, a full reconstruction of the trajectory within the muon system is performed to determine the drift velocity. In the first step, a pattern recognition algorithm is applied to identify hits belonging to the same track. Once the hits have been identified, the track is reconstructed under the assumption of a 54.3 μm/ns nominal drift velocity. In the second step the track is refit treating as free parameters the drift velocities at each hit and the time of passage of the muon through the chamber. The method is applied to the $r\phi$ view of the track segment in one chamber, where there are eight measured points in most cases. The z super-layers, where only four points are available, at most, are less significant for this analysis. The drift velocity is taken to be the mean value of the track-by-track drift-velocity distribution.

2010 JINST 5 T03016

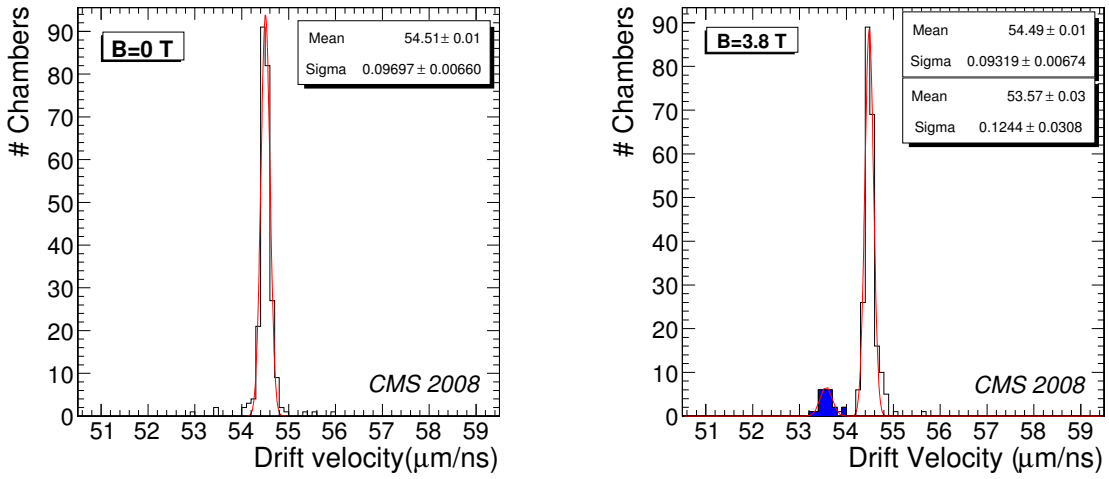

Figure 14. Drift velocities for $B = 0$ T (left) and $B = 3.8$ T (right). The small peak on the right panel corresponds to the MB1 chambers of Wheel +2 and Wheel -2, and shows the influence of a higher magnetic field in these regions.

Figure 13 shows the mean values of the drift velocity for the MB2 chambers of Wheel +2, using the mean-time method described in section 7 and the fit method described here. When using the mean-time method, the drift velocities have large systematic fluctuations from one sector to the other. This is related to the errors on the t_{trig} determination described in section 6, which cancel when the fit method is used.

The average drift-velocity values from the fit method, for all the chambers, are shown in figure 14, for runs without and with magnetic field (of 3.8 T).

The data at $B = 0$ T show an average value of 54.5 μm/ns for the drift velocity and a standard deviation indicating that differences between chambers are in the order of 0.2 %. For $B = 3.8$ T, a second peak is observed at 53.6 μm/ns. This peak corresponds to the MB1 chambers of the external wheels (Wheel +2 and Wheel -2) and is due to the presence of a higher radial magnetic field.

Similar values of the drift velocity have been obtained using the same calibration procedure applied to the simulated pp collision data. These results, presented in ref. [17], indicate that the calibration algorithm delivers a more uniform response in the case of collision data and that a large fraction of the fluctuations observed in the drift velocity calibration from CRAFT data may be attributed to the topology and timing of the cosmic ray events.

The effect on the drift velocity of the variation of the radial magnetic field along the z coordinate is shown in figure 15, as calculated with the fit method. Positive wheels (+1 and +2) are not in the figure but show the same behavior as their symmetric wheels (-1 and -2, respectively).

The presence of the radial component of the magnetic field affects, as expected, only the MB1 chambers, primarily in the external wheels but some effects are also observed in Wheels +1 and -1. The variation along z for the MB1 chambers of Wheels +2 and -2 is below 3 %, less than expected from the MTCC results [16], after taking into account the differences of the magnetic field conditions between both periods ($B = 4$ T during the MTCC in the surface hall, $B = 3.8$ T in the underground experimental hall).

This analysis of the drift velocity is very sensitive to the field strength and, in fact, provided

2010 JINST 5 T03016

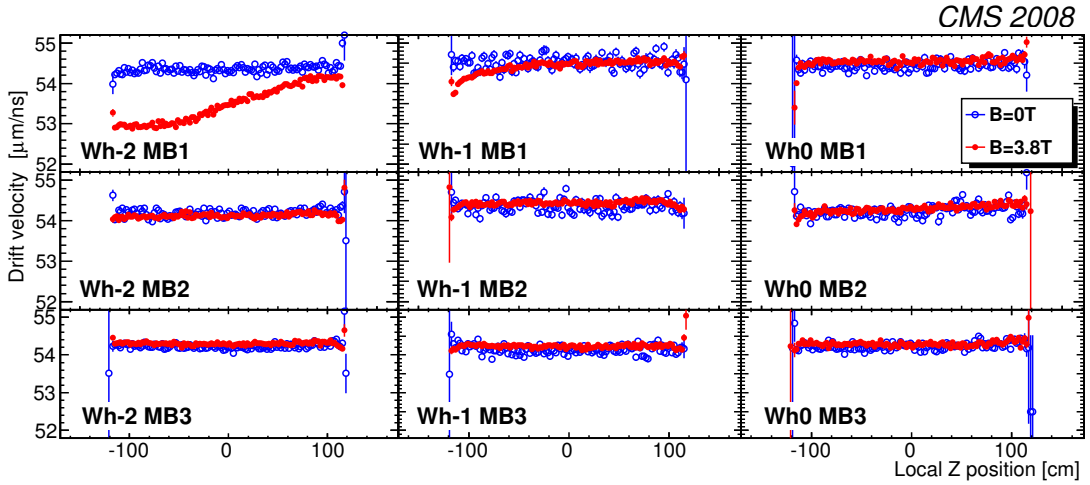

Figure 15. Drift velocities calculated using the muon track fit method described in this section. The values are shown as a function of the z position (measured by the z super-layers), and for $B = 0$ T and $B = 3.8$ T.

the first evidence of a systematic deviation from the true field strength in the field map. A new detailed calculation of the magnetic field has been performed [18], and the new analyses, currently in progress, show a z dependence in satisfactory agreement with the expectations.

All sectors in the same wheel show the same behavior, as illustrated in figure 16, where the values of the drift velocity along the z axis are shown for the MB1 chambers of some representative sectors of Wheels +2 and 0.

The drift velocity calculation, performed in this section, provides a better spatial resolution of the chambers with respect to the one obtained in section 7. This improvement is obtained with an extended track fit method which determines the drift velocity and the time of passage of the muon simultaneously with the regular track parameters. The detailed analysis of the spatial resolution for the cosmic ray data taking in 2008 is given in ref. [19]. The value obtained is about 250 μm, in fair agreement with the requirements for collision data [3].

10 Summary

This paper describes the calibration of the CMS Drift-Tubes system and presents results from the cosmic ray data-taking period which took place in 2008.

The complete calibration workflow has been applied to the data. It performed efficiently, monitoring the stability of the produced constants, and delivering with very low latency the calibration constants to the conditions database used by the offline reconstruction.

The first calibration step is the identification and masking of noisy channels to have a clean structure of the drift time distribution. The fraction of noisy cells was stable and about 0.01 %. The average noise rate was ~ 4 Hz.

The time pedestals, after having been corrected for the inter-channel synchronization, noisy channels, and the time of flight between upper and lower sectors, show a constant behavior in the entire DT system. Due to the particular topology of the cosmic ray events, the time pedestals are poorly defined for the sectors with chambers in the vertical plane, where cosmic ray tracks with

2010 JINST 5 T03016

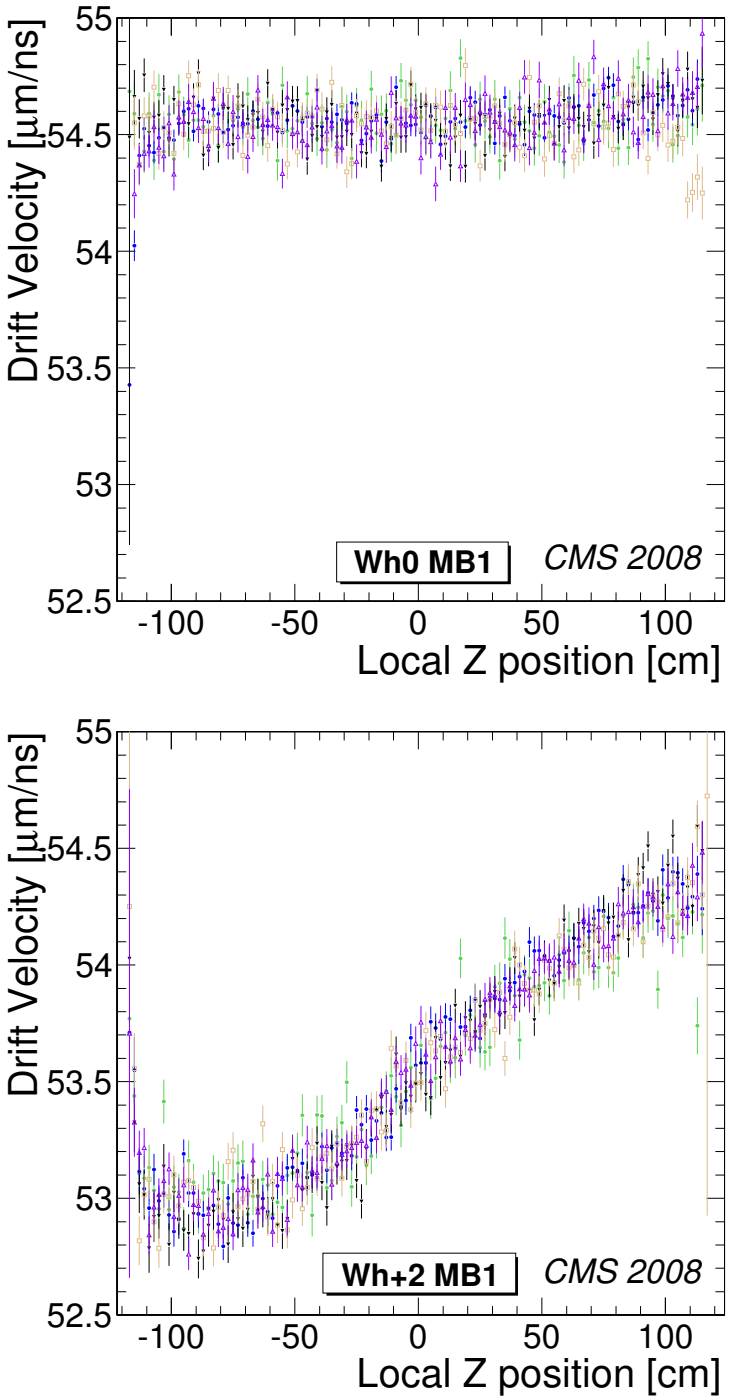

Figure 16. Drift velocities as a function of the local z position for MB1 chambers of some representative sectors of Wheel 0 (top) and Wheel +2 (bottom). Different sectors are indicated by different grey tones.

large impact angles are measured. For all the other sectors, an uncertainty of the order of 10 ns is observed. This value agrees with the uncertainty of the arrival time of cosmic ray muons within the clock cycle.

2010 JINST 5 T03016

The drift velocity calibration results show an approximately constant value of 54.3 μm/ns for all the chambers of the DT system, with a relative systematic uncertainty of 2.5 %. This uncertainty originates from the measured drift time, used in the mean-time method, which is limited by the uncertainty of the arrival time of cosmic ray muons. This explains why the obtained spatial resolution is worse than would be expected with collision data.

A more refined analysis of the drift velocity has been performed, exploiting the full potential of the CMS offline software for data reconstruction. It uses a track fitting procedure which leaves as free parameters the drift velocity and the time of passage of the muons through the chambers. Cosmic ray data with and without magnetic field have been studied. Without magnetic field, a constant average value of 54.5 μm/ns has been observed, with an error of 0.2 %; when the field strength is 3.8 T, the innermost chambers of the external barrel wheels measure a lower value, as expected, of about 53.6 μm/ns. These results confirm what was observed in an analysis performed on simulated collision data and provide a spatial resolution that is close to the design performance.

Acknowledgements

We thank the technical and administrative staff at CERN and other CMS Institutes, and acknowledge support from: FMSR (Austria); FNRS and FWO (Belgium); CNPq, CAPES, FAPERJ, and FAPESP (Brazil); MES (Bulgaria); CERN; CAS, MoST, and NSFC (China); COLCIENCIAS (Colombia); MSES (Croatia); RPF (Cyprus); Academy of Sciences and NICPB (Estonia); Academy of Finland, ME, and HIP (Finland); CEA and CNRS/IN2P3 (France); BMBF, DFG, and HGF (Germany); GSRT (Greece); OTKA and NKTH (Hungary); DAE and DST (India); IPM (Iran); SFI (Ireland); INFN (Italy); NRF (Korea); LAS (Lithuania); CINVESTAV, CONACYT, SEP, and UASLP-FAI (Mexico); PAEC (Pakistan); SCSR (Poland); FCT (Portugal); JINR (Armenia, Belarus, Georgia, Ukraine, Uzbekistan); MST and MAE (Russia); MSTDS (Serbia); MICINN and CPAN (Spain); Swiss Funding Agencies (Switzerland); NSC (Taipei); TUBITAK and TAEK (Turkey); STFC (United Kingdom); DOE and NSF (USA). Individuals have received support from the Marie-Curie IEF program (European Union); the Leventis Foundation; the A. P. Sloan Foundation; and the Alexander von Humboldt Foundation.

References

[1] CMS collaboration, *The CMS experiment at the CERN LHC*, 2008 *JINST* **3** S08004.

[2] L. Evans and P. Bryant eds., *LHC Machine*, 2008 *JINST* **3** S08001.

[3] CMS collaboration, *The Muon Project Technical Design Report*, CERN-LHCC-97-032 (1997).

[4] CMS collaboration, *Commissioning of the CMS experiment and the cosmic run at four tesla*, 2010 *JINST* **5** T03001.

[5] CMS collaboration, *Performance of the CMS drift-tube chamber local trigger with cosmic rays*, 2010 *JINST* **5** T03003.

[6] J. Christiansen, *High Performance Time to Digital Converter*, Version 2.1 CERN-EP-MIC (2002).

[7] G. Altenhoefer, *Development of a Drift Chamber for Drift Velocity Monitoring in the CMS Barrel Muon System*, Diploma Thesis, III Phys. Inst. A, RWTH Aachen (2006).

2010 JINST 5 T03016

[8] J. Frangenheim, *Measurements of the drift velocity using a small gas chamber for monitoring of the CMS muon system*, Diploma Thesis, III Phys. Inst. A, RWTH Aachen (2007).

[9] J. Puerta-Pelayo et al., *Parametrization of the Response of the Muon Barrel Drift Tubes*, CMS-NOTE-2005-018 (2005).

[10] G. Abbiendi et al., *Offline calibration procedure of the CMS drift tube detectors*, 2009 *JINST* **4** P05002.

[11] N. Amapane et al., *Local Muon Reconstruction in the Drift Tube Detectors*, CMS-NOTE-2009-008 (2009).

[12] D. Futyan et al., *The CMS Computing, Software and Analysis Challenge*, *Proceedings CHEP'09*, Prague, Czech Republic (2009).

[13] CMS collaboration, *CMS data processing workflows during an extended cosmic ray run*, 2010 *JINST* **5** T03006.

[14] L. Tuura et al., *CMS data quality monitoring:system and experiences*, *Proceedings CHEP'09*, Prague, Czech Republic (2009).

[15] M. Cerrada et al., *Results from the Analysis of the Test Beam Data taken with the Barrel Muon Prototype Q4*, CMS-NOTE-2001-041 (2001).

[16] M. Fouz et al., *Measurement of the Drift Velocity in the CMS Barrel Muon Chambers During the CMS Magnet Test and the Cosmic Challenge*, CMS-NOTE-2008-003 (2008).

[17] S. Maselli, *Calibration of the Barrel Muon Drift Tubes System in CMS*, *Proceedings CHEP'09*, Prague, Czech Republic (2009).

[18] CMS collaboration, *Precise mapping of the magnetic field in the CMS barrel yoke using cosmic rays*, 2010 *JINST* **5** T03021.

[19] CMS collaboration, *Performance of the CMS drift tube chambers with cosmic rays*, 2010 *JINST* **5** T03015.

2010 JINST 5 T03016

The CMS collaboration

Yerevan Physics Institute, Yerevan, Armenia
S. Chatrchyan, V. Khachatryan, A.M. Sirunyan

Institut für Hochenergiephysik der OeAW, Wien, Austria
W. Adam, B. Arnold, H. Bergauer, T. Bergauer, M. Dragicevic, M. Eichberger, J. Erö, M. Friedl, R. Frühwirth, V.M. Ghete, J. Hammer[1], S. Hänsel, M. Hoch, N. Hörmann, J. Hrubec, M. Jeitler, G. Kasieczka, K. Kastner, M. Krammer, D. Liko, I. Magrans de Abril, I. Mikulec, F. Mittermayr, B. Neuherz, M. Oberegger, M. Padrta, M. Pernicka, H. Rohringer, S. Schmid, R. Schöfbeck, T. Schreiner, R. Stark, H. Steininger, J. Strauss, A. Taurok, F. Teischinger, T. Themel, D. Uhl, P. Wagner, W. Waltenberger, G. Walzel, E. Widl, C.-E. Wulz

National Centre for Particle and High Energy Physics, Minsk, Belarus
V. Chekhovsky, O. Dvornikov, I. Emeliantchik, A. Litomin, V. Makarenko, I. Marfin, V. Mossolov, N. Shumeiko, A. Solin, R. Stefanovitch, J. Suarez Gonzalez, A. Tikhonov

Research Institute for Nuclear Problems, Minsk, Belarus
A. Fedorov, A. Karneyeu, M. Korzhik, V. Panov, R. Zuyeuski

Research Institute of Applied Physical Problems, Minsk, Belarus
P. Kuchinsky

Universiteit Antwerpen, Antwerpen, Belgium
W. Beaumont, L. Benucci, M. Cardaci, E.A. De Wolf, E. Delmeire, D. Druzhkin, M. Hashemi, X. Janssen, T. Maes, L. Mucibello, S. Ochesanu, R. Rougny, M. Selvaggi, H. Van Haevermaet, P. Van Mechelen, N. Van Remortel

Vrije Universiteit Brussel, Brussel, Belgium
V. Adler, S. Beauceron, S. Blyweert, J. D'Hondt, S. De Weirdt, O. Devroede, J. Heyninck, A. Kalogeropoulos, J. Maes, M. Maes, M.U. Mozer, S. Tavernier, W. Van Doninck[1], P. Van Mulders, I. Villella

Université Libre de Bruxelles, Bruxelles, Belgium
O. Bouhali, E.C. Chabert, O. Charaf, B. Clerbaux, G. De Lentdecker, V. Dero, S. Elgammal, A.P.R. Gay, G.H. Hammad, P.E. Marage, S. Rugovac, C. Vander Velde, P. Vanlaer, J. Wickens

Ghent University, Ghent, Belgium
M. Grunewald, B. Klein, A. Marinov, D. Ryckbosch, F. Thyssen, M. Tytgat, L. Vanelderen, P. Verwilligen

Université Catholique de Louvain, Louvain-la-Neuve, Belgium
S. Basegmez, G. Bruno, J. Caudron, C. Delaere, P. Demin, D. Favart, A. Giammanco, G. Grégoire, V. Lemaitre, O. Militaru, S. Ovyn, K. Piotrzkowski[1], L. Quertenmont, N. Schul

Université de Mons, Mons, Belgium
N. Beliy, E. Daubie

Centro Brasileiro de Pesquisas Fisicas, Rio de Janeiro, Brazil
G.A. Alves, M.E. Pol, M.H.G. Souza

2010 JINST 5 T03016

Universidade do Estado do Rio de Janeiro, Rio de Janeiro, Brazil
W. Carvalho, D. De Jesus Damiao, C. De Oliveira Martins, S. Fonseca De Souza, L. Mundim, V. Oguri, A. Santoro, S.M. Silva Do Amaral, A. Sznajder

Instituto de Fisica Teorica, Universidade Estadual Paulista, Sao Paulo, Brazil
T.R. Fernandez Perez Tomei, M.A. Ferreira Dias, E. M. Gregores[2], S.F. Novaes

Institute for Nuclear Research and Nuclear Energy, Sofia, Bulgaria
K. Abadjiev[1], T. Anguelov, J. Damgov, N. Darmenov[1], L. Dimitrov, V. Genchev[1], P. Iaydjiev, S. Piperov, S. Stoykova, G. Sultanov, R. Trayanov, I. Vankov

University of Sofia, Sofia, Bulgaria
A. Dimitrov, M. Dyulendarova, V. Kozhuharov, L. Litov, E. Marinova, M. Mateev, B. Pavlov, P. Petkov, Z. Toteva[1]

Institute of High Energy Physics, Beijing, China
G.M. Chen, H.S. Chen, W. Guan, C.H. Jiang, D. Liang, B. Liu, X. Meng, J. Tao, J. Wang, Z. Wang, Z. Xue, Z. Zhang

State Key Lab. of Nucl. Phys. and Tech., Peking University, Beijing, China
Y. Ban, J. Cai, Y. Ge, S. Guo, Z. Hu, Y. Mao, S.J. Qian, H. Teng, B. Zhu

Universidad de Los Andes, Bogota, Colombia
C. Avila, M. Baquero Ruiz, C.A. Carrillo Montoya, A. Gomez, B. Gomez Moreno, A.A. Ocampo Rios, A.F. Osorio Oliveros, D. Reyes Romero, J.C. Sanabria

Technical University of Split, Split, Croatia
N. Godinovic, K. Lelas, R. Plestina, D. Polic, I. Puljak

University of Split, Split, Croatia
Z. Antunovic, M. Dzelalija

Institute Rudjer Boskovic, Zagreb, Croatia
V. Brigljevic, S. Duric, K. Kadija, S. Morovic

University of Cyprus, Nicosia, Cyprus
R. Fereos, M. Galanti, J. Mousa, A. Papadakis, F. Ptochos, P.A. Razis, D. Tsiakkouri, Z. Zinonos

National Institute of Chemical Physics and Biophysics, Tallinn, Estonia
A. Hektor, M. Kadastik, K. Kannike, M. Müntel, M. Raidal, L. Rebane

Helsinki Institute of Physics, Helsinki, Finland
E. Anttila, S. Czellar, J. Härkönen, A. Heikkinen, V. Karimäki, R. Kinnunen, J. Klem, M.J. Kortelainen, T. Lampén, K. Lassila-Perini, S. Lehti, T. Lindén, P. Luukka, T. Mäenpää, J. Nysten, E. Tuominen, J. Tuominiemi, D. Ungaro, L. Wendland

Lappeenranta University of Technology, Lappeenranta, Finland
K. Banzuzi, A. Korpela, T. Tuuva

Laboratoire d'Annecy-le-Vieux de Physique des Particules, IN2P3-CNRS, Annecy-le-Vieux, France
P. Nedelec, D. Sillou

2010 JINST 5 T03016

DSM/IRFU, CEA/Saclay, Gif-sur-Yvette, France
M. Besancon, R. Chipaux, M. Dejardin, D. Denegri, J. Descamps, B. Fabbro, J.L. Faure, F. Ferri, S. Ganjour, F.X. Gentit, A. Givernaud, P. Gras, G. Hamel de Monchenault, P. Jarry, M.C. Lemaire, E. Locci, J. Malcles, M. Marionneau, L. Millischer, J. Rander, A. Rosowsky, D. Rousseau, M. Titov, P. Verrecchia

Laboratoire Leprince-Ringuet, Ecole Polytechnique, IN2P3-CNRS, Palaiseau, France
S. Baffioni, L. Bianchini, M. Bluj[3], P. Busson, C. Charlot, L. Dobrzynski, R. Granier de Cassagnac, M. Haguenauer, P. Miné, P. Paganini, Y. Sirois, C. Thiebaux, A. Zabi

Institut Pluridisciplinaire Hubert Curien, Université de Strasbourg, Université de Haute Alsace Mulhouse, CNRS/IN2P3, Strasbourg, France
J.-L. Agram[4], A. Besson, D. Bloch, D. Bodin, J.-M. Brom, E. Conte[4], F. Drouhin[4], J.-C. Fontaine[4], D. Gelé, U. Goerlach, L. Gross, P. Juillot, A.-C. Le Bihan, Y. Patois, J. Speck, P. Van Hove

Université de Lyon, Université Claude Bernard Lyon 1, CNRS-IN2P3, Institut de Physique Nucléaire de Lyon, Villeurbanne, France
C. Baty, M. Bedjidian, J. Blaha, G. Boudoul, H. Brun, N. Chanon, R. Chierici, D. Contardo, P. Depasse, T. Dupasquier, H. El Mamouni, F. Fassi[5], J. Fay, S. Gascon, B. Ille, T. Kurca, T. Le Grand, M. Lethuillier, N. Lumb, L. Mirabito, S. Perries, M. Vander Donckt, P. Verdier

E. Andronikashvili Institute of Physics, Academy of Science, Tbilisi, Georgia
N. Djaoshvili, N. Roinishvili, V. Roinishvili

Institute of High Energy Physics and Informatization, Tbilisi State University, Tbilisi, Georgia
N. Amaglobeli

RWTH Aachen University, I. Physikalisches Institut, Aachen, Germany
R. Adolphi, G. Anagnostou, R. Brauer, W. Braunschweig, M. Edelhoff, H. Esser, L. Feld, W. Karpinski, A. Khomich, K. Klein, N. Mohr, A. Ostaptchouk, D. Pandoulas, G. Pierschel, F. Raupach, S. Schael, A. Schultz von Dratzig, G. Schwering, D. Sprenger, M. Thomas, M. Weber, B. Wittmer, M. Wlochal

RWTH Aachen University, III. Physikalisches Institut A, Aachen, Germany
O. Actis, G. Altenhöfer, W. Bender, P. Biallass, M. Erdmann, G. Fetchenhauer[1], J. Frangenheim, T. Hebbeker, G. Hilgers, A. Hinzmann, K. Hoepfner, C. Hof, M. Kirsch, T. Klimkovich, P. Kreuzer[1], D. Lanske[†], M. Merschmeyer, A. Meyer, B. Philipps, H. Pieta, H. Reithler, S.A. Schmitz, L. Sonnenschein, M. Sowa, J. Steggemann, H. Szczesny, D. Teyssier, C. Zeidler

RWTH Aachen University, III. Physikalisches Institut B, Aachen, Germany
M. Bontenackels, M. Davids, M. Duda, G. Flügge, H. Geenen, M. Giffels, W. Haj Ahmad, T. Hermanns, D. Heydhausen, S. Kalinin, T. Kress, A. Linn, A. Nowack, L. Perchalla, M. Poettgens, O. Pooth, P. Sauerland, A. Stahl, D. Tornier, M.H. Zoeller

Deutsches Elektronen-Synchrotron, Hamburg, Germany
M. Aldaya Martin, U. Behrens, K. Borras, A. Campbell, E. Castro, D. Dammann, G. Eckerlin, A. Flossdorf, G. Flucke, A. Geiser, D. Hatton, J. Hauk, H. Jung, M. Kasemann, I. Katkov, C. Kleinwort, H. Kluge, A. Knutsson, E. Kuznetsova, W. Lange, W. Lohmann, R. Mankel[1],

2010 JINST 5 T03016

M. Marienfeld, A.B. Meyer, S. Miglioranzi, J. Mnich, M. Ohlerich, J. Olzem, A. Parenti, C. Rosemann, R. Schmidt, T. Schoerner-Sadenius, D. Volyanskyy, C. Wissing, W.D. Zeuner[1]

University of Hamburg, Hamburg, Germany

C. Autermann, F. Bechtel, J. Draeger, D. Eckstein, U. Gebbert, K. Kaschube, G. Kaussen, R. Klanner, B. Mura, S. Naumann-Emme, F. Nowak, U. Pein, C. Sander, P. Schleper, T. Schum, H. Stadie, G. Steinbrück, J. Thomsen, R. Wolf

Institut für Experimentelle Kernphysik, Karlsruhe, Germany

J. Bauer, P. Blüm, V. Buege, A. Cakir, T. Chwalek, W. De Boer, A. Dierlamm, G. Dirkes, M. Feindt, U. Felzmann, M. Frey, A. Furgeri, J. Gruschke, C. Hackstein, F. Hartmann[1], S. Heier, M. Heinrich, H. Held, D. Hirschbuehl, K.H. Hoffmann, S. Honc, C. Jung, T. Kuhr, T. Liamsuwan, D. Martschei, S. Mueller, Th. Müller, M.B. Neuland, M. Niegel, O. Oberst, A. Oehler, J. Ott, T. Peiffer, D. Piparo, G. Quast, K. Rabbertz, F. Ratnikov, N. Ratnikova, M. Renz, C. Saout[1], G. Sartisohn, A. Scheurer, P. Schieferdecker, F.-P. Schilling, G. Schott, H.J. Simonis, F.M. Stober, P. Sturm, D. Troendle, A. Trunov, W. Wagner, J. Wagner-Kuhr, M. Zeise, V. Zhukov[6], E.B. Ziebarth

Institute of Nuclear Physics "Demokritos", Aghia Paraskevi, Greece

G. Daskalakis, T. Geralis, K. Karafasoulis, A. Kyriakis, D. Loukas, A. Markou, C. Markou, C. Mavrommatis, E. Petrakou, A. Zachariadou

University of Athens, Athens, Greece

L. Gouskos, P. Katsas, A. Panagiotou[1]

University of Ioánnina, Ioánnina, Greece

I. Evangelou, P. Kokkas, N. Manthos, I. Papadopoulos, V. Patras, F.A. Triantis

KFKI Research Institute for Particle and Nuclear Physics, Budapest, Hungary

G. Bencze[1], L. Boldizsar, G. Debreczeni, C. Hajdu[1], S. Hernath, P. Hidas, D. Horvath[7], K. Krajczar, A. Laszlo, G. Patay, F. Sikler, N. Toth, G. Vesztergombi

Institute of Nuclear Research ATOMKI, Debrecen, Hungary

N. Beni, G. Christian, J. Imrek, J. Molnar, D. Novak, J. Palinkas, G. Szekely, Z. Szillasi[1], K. Tokesi, V. Veszpremi

University of Debrecen, Debrecen, Hungary

A. Kapusi, G. Marian, P. Raics, Z. Szabo, Z.L. Trocsanyi, B. Ujvari, G. Zilizi

Panjab University, Chandigarh, India

S. Bansal, H.S. Bawa, S.B. Beri, V. Bhatnagar, M. Jindal, M. Kaur, R. Kaur, J.M. Kohli, M.Z. Mehta, N. Nishu, L.K. Saini, A. Sharma, A. Singh, J.B. Singh, S.P. Singh

University of Delhi, Delhi, India

S. Ahuja, S. Arora, S. Bhattacharya[8], S. Chauhan, B.C. Choudhary, P. Gupta, S. Jain, S. Jain, M. Jha, A. Kumar, K. Ranjan, R.K. Shivpuri, A.K. Srivastava

Bhabha Atomic Research Centre, Mumbai, India

R.K. Choudhury, D. Dutta, S. Kailas, S.K. Kataria, A.K. Mohanty, L.M. Pant, P. Shukla, A. Topkar

Tata Institute of Fundamental Research - EHEP, Mumbai, India

T. Aziz, M. Guchait[9], A. Gurtu, M. Maity[10], D. Majumder, G. Majumder, K. Mazumdar, A. Nayak, A. Saha, K. Sudhakar

2010 JINST 5 T03016

Tata Institute of Fundamental Research - HECR, Mumbai, India
S. Banerjee, S. Dugad, N.K. Mondal

Institute for Studies in Theoretical Physics & Mathematics (IPM), Tehran, Iran
H. Arfaei, H. Bakhshiansohi, A. Fahim, A. Jafari, M. Mohammadi Najafabadi, A. Moshaii, S. Paktinat Mehdiabadi, S. Rouhani, B. Safarzadeh, M. Zeinali

University College Dublin, Dublin, Ireland
M. Felcini

INFN Sezione di Bari [a], Università di Bari [b], Politecnico di Bari [c], Bari, Italy
M. Abbrescia[a,b], L. Barbone[a], F. Chiumarulo[a], A. Clemente[a], A. Colaleo[a], D. Creanza[a,c], G. Cuscela[a], N. De Filippis[a], M. De Palma[a,b], G. De Robertis[a], G. Donvito[a], F. Fedele[a], L. Fiore[a], M. Franco[a], G. Iaselli[a,c], N. Lacalamita[a], F. Loddo[a], L. Lusito[a,b], G. Maggi[a,c], M. Maggi[a], N. Manna[a,b], B. Marangelli[a,b], S. My[a,c], S. Natali[a,b], S. Nuzzo[a,b], G. Papagni[a], S. Piccolomo[a], G.A. Pierro[a], C. Pinto[a], A. Pompili[a,b], G. Pugliese[a,c], R. Rajan[a], A. Ranieri[a], F. Romano[a,c], G. Roselli[a,b], G. Selvaggi[a,b], Y. Shinde[a], L. Silvestris[a], S. Tupputi[a,b], G. Zito[a]

INFN Sezione di Bologna [a], Universita di Bologna [b], Bologna, Italy
G. Abbiendi[a], W. Bacchi[a,b], A.C. Benvenuti[a], M. Boldini[a], D. Bonacorsi[a], S. Braibant-Giacomelli[a,b], V.D. Cafaro[a], S.S. Caiazza[a], P. Capiluppi[a,b], A. Castro[a,b], F.R. Cavallo[a], G. Codispoti[a,b], M. Cuffiani[a,b], I. D'Antone[a], G.M. Dallavalle[a,1], F. Fabbri[a], A. Fanfani[a,b], D. Fasanella[a], P. Giacomelli[a], V. Giordano[a], M. Giunta[a,1], C. Grandi[a], M. Guerzoni[a], S. Marcellini[a], G. Masetti[a,b], A. Montanari[a], F.L. Navarria[a,b], F. Odorici[a], G. Pellegrini[a], A. Perrotta[a], A.M. Rossi[a,b], T. Rovelli[a,b], G. Siroli[a,b], G. Torromeo[a], R. Travaglini[a,b]

INFN Sezione di Catania [a], Universita di Catania [b], Catania, Italy
S. Albergo[a,b], S. Costa[a,b], R. Potenza[a,b], A. Tricomi[a,b], C. Tuve[a]

INFN Sezione di Firenze [a], Universita di Firenze [b], Firenze, Italy
G. Barbagli[a], G. Broccolo[a,b], V. Ciulli[a,b], C. Civinini[a], R. D'Alessandro[a,b], E. Focardi[a,b], S. Frosali[a,b], E. Gallo[a], C. Genta[a,b], G. Landi[a,b], P. Lenzi[a,b,1], M. Meschini[a], S. Paoletti[a], G. Sguazzoni[a], A. Tropiano[a]

INFN Laboratori Nazionali di Frascati, Frascati, Italy
L. Benussi, M. Bertani, S. Bianco, S. Colafranceschi[11], D. Colonna[11], F. Fabbri, M. Giardoni, L. Passamonti, D. Piccolo, D. Pierluigi, B. Ponzio, A. Russo

INFN Sezione di Genova, Genova, Italy
P. Fabbricatore, R. Musenich

INFN Sezione di Milano-Biccoca [a], Universita di Milano-Bicocca [b], Milano, Italy
A. Benaglia[a], M. Calloni[a], G.B. Cerati[a,b,1], P. D'Angelo[a], F. De Guio[a], F.M. Farina[a], A. Ghezzi[a], P. Govoni[a,b], M. Malberti[a,b,1], S. Malvezzi[a], A. Martelli[a], D. Menasce[a], V. Miccio[a,b], L. Moroni[a], P. Negri[a,b], M. Paganoni[a,b], D. Pedrini[a], A. Pullia[a,b], S. Ragazzi[a,b], N. Redaelli[a], S. Sala[a], R. Salerno[a,b], T. Tabarelli de Fatis[a,b], V. Tancini[a,b], S. Taroni[a,b]

INFN Sezione di Napoli [a], Universita di Napoli "Federico II" [b], Napoli, Italy
S. Buontempo[a], N. Cavallo[a], A. Cimmino[a,b,1], M. De Gruttola[a,b,1], F. Fabozzi[a,12], A.O.M. Iorio[a], L. Lista[a], D. Lomidze[a], P. Noli[a,b], P. Paolucci[a], C. Sciacca[a,b]

2010 JINST 5 T03016

INFN Sezione di Padova [a], Università di Padova [b], Padova, Italy
P. Azzi[a,1], N. Bacchetta[a], L. Barcellan[a], P. Bellan[a,b,1], M. Bellato[a], M. Benettoni[a], M. Biasotto[a,13], D. Bisello[a,b], E. Borsato[a,b], A. Branca[a], R. Carlin[a,b], L. Castellani[a], P. Checchia[a], E. Conti[a], F. Dal Corso[a], M. De Mattia[a,b], T. Dorigo[a], U. Dosselli[a], F. Fanzago[a], F. Gasparini[a,b], U. Gasparini[a,b], P. Giubilato[a,b], F. Gonella[a], A. Gresele[a,14], M. Gulmini[a,13], A. Kaminskiy[a,b], S. Lacaprara[a,13], I. Lazzizzera[a,14], M. Margoni[a,b], G. Maron[a,13], S. Mattiazzo[a,b], M. Mazzucato[a], M. Meneghelli[a], A.T. Meneguzzo[a,b], M. Michelotto[a], F. Montecassiano[a], M. Nespolo[a], M. Passaseo[a], M. Pegoraro[a], L. Perrozzi[a], N. Pozzobon[a,b], P. Ronchese[a,b], F. Simonetto[a,b], N. Toniolo[a], E. Torassa[a], M. Tosi[a,b], A. Triossi[a], S. Vanini[a,b], S. Ventura[a], P. Zotto[a,b], G. Zumerle[a,b]

INFN Sezione di Pavia [a], Universita di Pavia [b], Pavia, Italy
P. Baesso[a,b], U. Berzano[a], S. Bricola[a], M.M. Necchi[a,b], D. Pagano[a,b], S.P. Ratti[a,b], C. Riccardi[a,b], P. Torre[a,b], A. Vicini[a], P. Vitulo[a,b], C. Viviani[a,b]

INFN Sezione di Perugia [a], Universita di Perugia [b], Perugia, Italy
D. Aisa[a], S. Aisa[a], E. Babucci[a], M. Biasini[a,b], G.M. Bilei[a], B. Caponeri[a,b], B. Checcucci[a], N. Dinu[a], L. Fanò[a], L. Farnesini[a], P. Lariccia[a,b], A. Lucaroni[a,b], G. Mantovani[a,b], A. Nappi[a,b], A. Piluso[a], V. Postolache[a], A. Santocchia[a,b], L. Servoli[a], D. Tonoiu[a], A. Vedaee[a], R. Volpe[a,b]

INFN Sezione di Pisa [a], Universita di Pisa [b], Scuola Normale Superiore di Pisa [c], Pisa, Italy
P. Azzurri[a,c], G. Bagliesi[a], J. Bernardini[a,b], L. Berretta[a], T. Boccali[a], A. Bocci[a,c], L. Borrello[a,c], F. Bosi[a], F. Calzolari[a], R. Castaldi[a], R. Dell'Orso[a], F. Fiori[a,b], L. Foà[a,c], S. Gennai[a,c], A. Giassi[a], A. Kraan[a], F. Ligabue[a,c], T. Lomtadze[a], F. Mariani[a], L. Martini[a], M. Massa[a], A. Messineo[a,b], A. Moggi[a], F. Palla[a], F. Palmonari[a], G. Petragnani[a], G. Petrucciani[a,c], F. Raffaelli[a], S. Sarkar[a], G. Segneri[a], A.T. Serban[a], P. Spagnolo[a,1], R. Tenchini[a,1], S. Tolaini[a], G. Tonelli[a,b,1], A. Venturi[a], P.G. Verdini[a]

INFN Sezione di Roma [a], Universita di Roma "La Sapienza" [b], Roma, Italy
S. Baccaro[a,15], L. Barone[a,b], A. Bartoloni[a], F. Cavallari[a,1], I. Dafinei[a], D. Del Re[a,b], E. Di Marco[a,b], M. Diemoz[a], D. Franci[a,b], E. Longo[a,b], G. Organtini[a,b], A. Palma[a,b], F. Pandolfi[a,b], R. Paramatti[a,1], F. Pellegrino[a], S. Rahatlou[a,b], C. Rovelli[a]

INFN Sezione di Torino [a], Università di Torino [b], Università del Piemonte Orientale (Novara) [c], Torino, Italy
G. Alampi[a], N. Amapane[a,b], R. Arcidiacono[a,b], S. Argiro[a,b], M. Arneodo[a,c], C. Biino[a], M.A. Borgia[a,b], C. Botta[a,b], N. Cartiglia[a], R. Castello[a,b], G. Cerminara[a,b], M. Costa[a,b], D. Dattola[a], G. Dellacasa[a], N. Demaria[a], G. Dughera[a], F. Dumitrache[a], A. Graziano[a,b], C. Mariotti[a], M. Marone[a,b], S. Maselli[a], E. Migliore[a,b], G. Mila[a,b], V. Monaco[a,b], M. Musich[a,b], M. Nervo[a,b], M.M. Obertino[a,c], S. Oggero[a,b], R. Panero[a], N. Pastrone[a], M. Pelliccioni[a,b], A. Romero[a,b], M. Ruspa[a,c], R. Sacchi[a,b], A. Solano[a,b], A. Staiano[a], P.P. Trapani[a,b,1], D. Trocino[a,b], A. Vilela Pereira[a,b], L. Visca[a,b], A. Zampieri[a]

INFN Sezione di Trieste [a], Universita di Trieste [b], Trieste, Italy
F. Ambroglini[a,b], S. Belforte[a], F. Cossutti[a], G. Della Ricca[a,b], B. Gobbo[a], A. Penzo[a]

Kyungpook National University, Daegu, Korea
S. Chang, J. Chung, D.H. Kim, G.N. Kim, D.J. Kong, H. Park, D.C. Son

2010 JINST 5 T03016

Wonkwang University, Iksan, Korea
S.Y. Bahk

Chonnam National University, Kwangju, Korea
S. Song

Konkuk University, Seoul, Korea
S.Y. Jung

Korea University, Seoul, Korea
B. Hong, H. Kim, J.H. Kim, K.S. Lee, D.H. Moon, S.K. Park, H.B. Rhee, K.S. Sim

Seoul National University, Seoul, Korea
J. Kim

University of Seoul, Seoul, Korea
M. Choi, G. Hahn, I.C. Park

Sungkyunkwan University, Suwon, Korea
S. Choi, Y. Choi, J. Goh, H. Jeong, T.J. Kim, J. Lee, S. Lee

Vilnius University, Vilnius, Lithuania
M. Janulis, D. Martisiute, P. Petrov, T. Sabonis

Centro de Investigacion y de Estudios Avanzados del IPN, Mexico City, Mexico
H. Castilla Valdez[1], A. Sánchez Hernández

Universidad Iberoamericana, Mexico City, Mexico
S. Carrillo Moreno

Universidad Autónoma de San Luis Potosí, San Luis Potosí, Mexico
A. Morelos Pineda

University of Auckland, Auckland, New Zealand
P. Allfrey, R.N.C. Gray, D. Krofcheck

University of Canterbury, Christchurch, New Zealand
N. Bernardino Rodrigues, P.H. Butler, T. Signal, J.C. Williams

National Centre for Physics, Quaid-I-Azam University, Islamabad, Pakistan
M. Ahmad, I. Ahmed, W. Ahmed, M.I. Asghar, M.I.M. Awan, H.R. Hoorani, I. Hussain, W.A. Khan, T. Khurshid, S. Muhammad, S. Qazi, H. Shahzad

Institute of Experimental Physics, Warsaw, Poland
M. Cwiok, R. Dabrowski, W. Dominik, K. Doroba, M. Konecki, J. Krolikowski, K. Pozniak[16], R. Romaniuk, W. Zabolotny[16], P. Zych

Soltan Institute for Nuclear Studies, Warsaw, Poland
T. Frueboes, R. Gokieli, L. Goscilo, M. Górski, M. Kazana, K. Nawrocki, M. Szleper, G. Wrochna, P. Zalewski

Laboratório de Instrumentação e Física Experimental de Partículas, Lisboa, Portugal
N. Almeida, L. Antunes Pedro, P. Bargassa, A. David, P. Faccioli, P.G. Ferreira Parracho, M. Freitas Ferreira, M. Gallinaro, M. Guerra Jordao, P. Martins, G. Mini, P. Musella, J. Pela, L. Raposo, P.Q. Ribeiro, S. Sampaio, J. Seixas, J. Silva, P. Silva, D. Soares, M. Sousa, J. Varela, H.K. Wöhri

2010 JINST 5 T03016

Joint Institute for Nuclear Research, Dubna, Russia
I. Altsybeev, I. Belotelov, P. Bunin, Y. Ershov, I. Filozova, M. Finger, M. Finger Jr., A. Golunov, I. Golutvin, N. Gorbounov, V. Kalagin, A. Kamenev, V. Karjavin, V. Konoplyanikov, V. Korenkov, G. Kozlov, A. Kurenkov, A. Lanev, A. Makankin, V.V. Mitsyn, P. Moisenz, E. Nikonov, D. Oleynik, V. Palichik, V. Perelygin, A. Petrosyan, R. Semenov, S. Shmatov, V. Smirnov, D. Smolin, E. Tikhonenko, S. Vasil'ev, A. Vishnevskiy, A. Volodko, A. Zarubin, V. Zhiltsov

Petersburg Nuclear Physics Institute, Gatchina (St Petersburg), Russia
N. Bondar, L. Chtchipounov, A. Denisov, Y. Gavrikov, G. Gavrilov, V. Golovtsov, Y. Ivanov, V. Kim, V. Kozlov, P. Levchenko, G. Obrant, E. Orishchin, A. Petrunin, Y. Shcheglov, A. Shchetkovskiy, V. Sknar, I. Smirnov, V. Sulimov, V. Tarakanov, L. Uvarov, S. Vavilov, G. Velichko, S. Volkov, A. Vorobyev

Institute for Nuclear Research, Moscow, Russia
Yu. Andreev, A. Anisimov, P. Antipov, A. Dermenev, S. Gninenko, N. Golubev, M. Kirsanov, N. Krasnikov, V. Matveev, A. Pashenkov, V.E. Postoev, A. Solovey, A. Solovey, A. Toropin, S. Troitsky

Institute for Theoretical and Experimental Physics, Moscow, Russia
A. Baud, V. Epshteyn, V. Gavrilov, N. Ilina, V. Kaftanov†, V. Kolosov, M. Kossov[1], A. Krokhotin, S. Kuleshov, A. Oulianov, G. Safronov, S. Semenov, I. Shreyber, V. Stolin, E. Vlasov, A. Zhokin

Moscow State University, Moscow, Russia
E. Boos, M. Dubinin[17], L. Dudko, A. Ershov, A. Gribushin, V. Klyukhin, O. Kodolova, I. Lokhtin, S. Petrushanko, L. Sarycheva, V. Savrin, A. Snigirev, I. Vardanyan

P.N. Lebedev Physical Institute, Moscow, Russia
I. Dremin, M. Kirakosyan, N. Konovalova, S.V. Rusakov, A. Vinogradov

State Research Center of Russian Federation, Institute for High Energy Physics, Protvino, Russia
S. Akimenko, A. Artamonov, I. Azhgirey, S. Bitioukov, V. Burtovoy, V. Grishin[1], V. Kachanov, D. Konstantinov, V. Krychkine, A. Levine, I. Lobov, V. Lukanin, Y. Mel'nik, V. Petrov, R. Ryutin, S. Slabospitsky, A. Sobol, A. Sytine, L. Tourtchanovitch, S. Troshin, N. Tyurin, A. Uzunian, A. Volkov

Vinca Institute of Nuclear Sciences, Belgrade, Serbia
P. Adzic, M. Djordjevic, D. Jovanovic[18], D. Krpic[18], D. Maletic, J. Puzovic[18], N. Smiljkovic

Centro de Investigaciones Energéticas Medioambientales y Tecnológicas (CIEMAT), Madrid, Spain
M. Aguilar-Benitez, J. Alberdi, J. Alcaraz Maestre, P. Arce, J.M. Barcala, C. Battilana, C. Burgos Lazaro, J. Caballero Bejar, E. Calvo, M. Cardenas Montes, M. Cepeda, M. Cerrada, M. Chamizo Llatas, F. Clemente, N. Colino, M. Daniel, B. De La Cruz, A. Delgado Peris, C. Diez Pardos, C. Fernandez Bedoya, J.P. Fernández Ramos, A. Ferrando, J. Flix, M.C. Fouz, P. Garcia-Abia, A.C. Garcia-Bonilla, O. Gonzalez Lopez, S. Goy Lopez, J.M. Hernandez, M.I. Josa, J. Marin, G. Merino, J. Molina, A. Molinero, J.J. Navarrete, J.C. Oller, J. Puerta Pelayo, L. Romero, J. Santaolalla, C. Villanueva Munoz, C. Willmott, C. Yuste

2010 JINST 5 T03016

Universidad Autónoma de Madrid, Madrid, Spain
C. Albajar, M. Blanco Otano, J.F. de Trocóniz, A. Garcia Raboso, J.O. Lopez Berengueres

Universidad de Oviedo, Oviedo, Spain
J. Cuevas, J. Fernandez Menendez, I. Gonzalez Caballero, L. Lloret Iglesias, H. Naves Sordo, J.M. Vizan Garcia

Instituto de Física de Cantabria (IFCA), CSIC-Universidad de Cantabria, Santander, Spain
I.J. Cabrillo, A. Calderon, S.H. Chuang, I. Diaz Merino, C. Diez Gonzalez, J. Duarte Campderros, M. Fernandez, G. Gomez, J. Gonzalez Sanchez, R. Gonzalez Suarez, C. Jorda, P. Lobelle Pardo, A. Lopez Virto, J. Marco, R. Marco, C. Martinez Rivero, P. Martinez Ruiz del Arbol, F. Matorras, T. Rodrigo, A. Ruiz Jimeno, L. Scodellaro, M. Sobron Sanudo, I. Vila, R. Vilar Cortabitarte

CERN, European Organization for Nuclear Research, Geneva, Switzerland
D. Abbaneo, E. Albert, M. Alidra, S. Ashby, E. Auffray, J. Baechler, P. Baillon, A.H. Ball, S.L. Bally, D. Barney, F. Beaudette[19], R. Bellan, D. Benedetti, G. Benelli, C. Bernet, P. Bloch, S. Bolognesi, M. Bona, J. Bos, N. Bourgeois, T. Bourrel, H. Breuker, K. Bunkowski, D. Campi, T. Camporesi, E. Cano, A. Cattai, J.P. Chatelain, M. Chauvey, T. Christiansen, J.A. Coarasa Perez, A. Conde Garcia, R. Covarelli, B. Curé, A. De Roeck, V. Delachenal, D. Deyrail, S. Di Vincenzo[20], S. Dos Santos, T. Dupont, L.M. Edera, A. Elliott-Peisert, M. Eppard, M. Favre, N. Frank, W. Funk, A. Gaddi, M. Gastal, M. Gateau, H. Gerwig, D. Gigi, K. Gill, D. Giordano, J.P. Girod, F. Glege, R. Gomez-Reino Garrido, R. Goudard, S. Gowdy, R. Guida, L. Guiducci, J. Gutleber, M. Hansen, C. Hartl, J. Harvey, B. Hegner, H.F. Hoffmann, A. Holzner, A. Honma, M. Huhtinen, V. Innocente, P. Janot, G. Le Godec, P. Lecoq, C. Leonidopoulos, R. Loos, C. Lourenço, A. Lyonnet, A. Macpherson, N. Magini, J.D. Maillefaud, G. Maire, T. Mäki, L. Malgeri, M. Mannelli, L. Masetti, F. Meijers, P. Meridiani, S. Mersi, E. Meschi, A. Meynet Cordonnier, R. Moser, M. Mulders, J. Mulon, M. Noy, A. Oh, G. Olesen, A. Onnela, T. Orimoto, L. Orsini, E. Perez, G. Perinic, J.F. Pernot, P. Petagna, P. Petiot, A. Petrilli, A. Pfeiffer, M. Pierini, M. Pimiä, R. Pintus, B. Pirollet, H. Postema, A. Racz, S. Ravat, S.B. Rew, J. Rodrigues Antunes, G. Rolandi[21], M. Rovere, V. Ryjov, H. Sakulin, D. Samyn, H. Sauce, C. Schäfer, W.D. Schlatter, M. Schröder, C. Schwick, A. Sciaba, I. Segoni, A. Sharma, N. Siegrist, P. Siegrist, N. Sinanis, T. Sobrier, P. Sphicas[22], D. Spiga, M. Spiropulu[17], F. Stöckli, P. Traczyk, P. Tropea, J. Troska, A. Tsirou, L. Veillet, G.I. Veres, M. Voutilainen, P. Wertelaers, M. Zanetti

Paul Scherrer Institut, Villigen, Switzerland
W. Bertl, K. Deiters, W. Erdmann, K. Gabathuler, R. Horisberger, Q. Ingram, H.C. Kaestli, S. König, D. Kotlinski, U. Langenegger, F. Meier, D. Renker, T. Rohe, J. Sibille[23], A. Starodumov[24]

Institute for Particle Physics, ETH Zurich, Zurich, Switzerland
B. Betev, L. Caminada[25], Z. Chen, S. Cittolin, D.R. Da Silva Di Calafiori, S. Dambach[25], G. Dissertori, M. Dittmar, C. Eggel[25], J. Eugster, G. Faber, K. Freudenreich, C. Grab, A. Hervé, W. Hintz, P. Lecomte, P.D. Luckey, W. Lustermann, C. Marchica[25], P. Milenovic[26], F. Moortgat, A. Nardulli, F. Nessi-Tedaldi, L. Pape, F. Pauss, T. Punz, A. Rizzi, F.J. Ronga, L. Sala, A.K. Sanchez, M.-C. Sawley, V. Sordini, B. Stieger, L. Tauscher†, A. Thea, K. Theofilatos, D. Treille, P. Trüb[25], M. Weber, L. Wehrli, J. Weng, S. Zelepoukine[27]

2010 JINST 5 T03016

Universität Zürich, Zurich, Switzerland
C. Amsler, V. Chiochia, S. De Visscher, C. Regenfus, P. Robmann, T. Rommerskirchen, A. Schmidt, D. Tsirigkas, L. Wilke

National Central University, Chung-Li, Taiwan
Y.H. Chang, E.A. Chen, W.T. Chen, A. Go, C.M. Kuo, S.W. Li, W. Lin

National Taiwan University (NTU), Taipei, Taiwan
P. Bartalini, P. Chang, Y. Chao, K.F. Chen, W.-S. Hou, Y. Hsiung, Y.J. Lei, S.W. Lin, R.-S. Lu, J. Schümann, J.G. Shiu, Y.M. Tzeng, K. Ueno, Y. Velikzhanin, C.C. Wang, M. Wang

Cukurova University, Adana, Turkey
A. Adiguzel, A. Ayhan, A. Azman Gokce, M.N. Bakirci, S. Cerci, I. Dumanoglu, E. Eskut, S. Girgis, E. Gurpinar, I. Hos, T. Karaman, T. Karaman, A. Kayis Topaksu, P. Kurt, G. Önengüt, G. Önengüt Gökbulut, K. Ozdemir, S. Ozturk, A. Polatöz, K. Sogut[28], B. Tali, H. Topakli, D. Uzun, L.N. Vergili, M. Vergili

Middle East Technical University, Physics Department, Ankara, Turkey
I.V. Akin, T. Aliev, S. Bilmis, M. Deniz, H. Gamsizkan, A.M. Guler, K. Öcalan, M. Serin, R. Sever, U.E. Surat, M. Zeyrek

Bogaziçi University, Department of Physics, Istanbul, Turkey
M. Deliomeroglu, D. Demir[29], E. Gülmez, A. Halu, B. Isildak, M. Kaya[30], O. Kaya[30], S. Ozkorucuklu[31], N. Sonmez[32]

National Scientific Center, Kharkov Institute of Physics and Technology, Kharkov, Ukraine
L. Levchuk, S. Lukyanenko, D. Soroka, S. Zub

University of Bristol, Bristol, United Kingdom
F. Bostock, J.J. Brooke, T.L. Cheng, D. Cussans, R. Frazier, J. Goldstein, N. Grant, M. Hansen, G.P. Heath, H.F. Heath, C. Hill, B. Huckvale, J. Jackson, C.K. Mackay, S. Metson, D.M. Newbold[33], K. Nirunpong, V.J. Smith, J. Velthuis, R. Walton

Rutherford Appleton Laboratory, Didcot, United Kingdom
K.W. Bell, C. Brew, R.M. Brown, B. Camanzi, D.J.A. Cockerill, J.A. Coughlan, N.I. Geddes, K. Harder, S. Harper, B.W. Kennedy, P. Murray, C.H. Shepherd-Themistocleous, I.R. Tomalin, J.H. Williams†, W.J. Womersley, S.D. Worm

Imperial College, University of London, London, United Kingdom
R. Bainbridge, G. Ball, J. Ballin, R. Beuselinck, O. Buchmuller, D. Colling, N. Cripps, G. Davies, M. Della Negra, C. Foudas, J. Fulcher, D. Futyan, G. Hall, J. Hays, G. Iles, G. Karapostoli, B.C. MacEvoy, A.-M. Magnan, J. Marrouche, J. Nash, A. Nikitenko[24], A. Papageorgiou, M. Pesaresi, K. Petridis, M. Pioppi[34], D.M. Raymond, N. Rompotis, A. Rose, M.J. Ryan, C. Seez, P. Sharp, G. Sidiropoulos[1], M. Stettler, M. Stoye, M. Takahashi, A. Tapper, C. Timlin, S. Tourneur, M. Vazquez Acosta, T. Virdee[1], S. Wakefield, D. Wardrope, T. Whyntie, M. Wingham

Brunel University, Uxbridge, United Kingdom
J.E. Cole, I. Goitom, P.R. Hobson, A. Khan, P. Kyberd, D. Leslie, C. Munro, I.D. Reid, C. Siamitros, R. Taylor, L. Teodorescu, I. Yaselli

2010 JINST 5 T03016

Boston University, Boston, U.S.A.
T. Bose, M. Carleton, E. Hazen, A.H. Heering, A. Heister, J. St. John, P. Lawson, D. Lazic, D. Osborne, J. Rohlf, L. Sulak, S. Wu

Brown University, Providence, U.S.A.
J. Andrea, A. Avetisyan, S. Bhattacharya, J.P. Chou, D. Cutts, S. Esen, G. Kukartsev, G. Landsberg, M. Narain, D. Nguyen, T. Speer, K.V. Tsang

University of California, Davis, Davis, U.S.A.
R. Breedon, M. Calderon De La Barca Sanchez, M. Case, D. Cebra, M. Chertok, J. Conway, P.T. Cox, J. Dolen, R. Erbacher, E. Friis, W. Ko, A. Kopecky, R. Lander, A. Lister, H. Liu, S. Maruyama, T. Miceli, M. Nikolic, D. Pellett, J. Robles, M. Searle, J. Smith, M. Squires, J. Stilley, M. Tripathi, R. Vasquez Sierra, C. Veelken

University of California, Los Angeles, Los Angeles, U.S.A.
V. Andreev, K. Arisaka, D. Cline, R. Cousins, S. Erhan[1], J. Hauser, M. Ignatenko, C. Jarvis, J. Mumford, C. Plager, G. Rakness, P. Schlein[†], J. Tucker, V. Valuev, R. Wallny, X. Yang

University of California, Riverside, Riverside, U.S.A.
J. Babb, M. Bose, A. Chandra, R. Clare, J.A. Ellison, J.W. Gary, G. Hanson, G.Y. Jeng, S.C. Kao, F. Liu, H. Liu, A. Luthra, H. Nguyen, G. Pasztor[35], A. Satpathy, B.C. Shen[†], R. Stringer, J. Sturdy, V. Sytnik, R. Wilken, S. Wimpenny

University of California, San Diego, La Jolla, U.S.A.
J.G. Branson, E. Dusinberre, D. Evans, F. Golf, R. Kelley, M. Lebourgeois, J. Letts, E. Lipeles, B. Mangano, J. Muelmenstaedt, M. Norman, S. Padhi, A. Petrucci, H. Pi, M. Pieri, R. Ranieri, M. Sani, V. Sharma, S. Simon, F. Würthwein, A. Yagil

University of California, Santa Barbara, Santa Barbara, U.S.A.
C. Campagnari, M. D'Alfonso, T. Danielson, J. Garberson, J. Incandela, C. Justus, P. Kalavase, S.A. Koay, D. Kovalskyi, V. Krutelyov, J. Lamb, S. Lowette, V. Pavlunin, F. Rebassoo, J. Ribnik, J. Richman, R. Rossin, D. Stuart, W. To, J.R. Vlimant, M. Witherell

California Institute of Technology, Pasadena, U.S.A.
A. Apresyan, A. Bornheim, J. Bunn, M. Chiorboli, M. Gataullin, D. Kcira, V. Litvine, Y. Ma, H.B. Newman, C. Rogan, V. Timciuc, J. Veverka, R. Wilkinson, Y. Yang, L. Zhang, K. Zhu, R.Y. Zhu

Carnegie Mellon University, Pittsburgh, U.S.A.
B. Akgun, R. Carroll, T. Ferguson, D.W. Jang, S.Y. Jun, M. Paulini, J. Russ, N. Terentyev, H. Vogel, I. Vorobiev

University of Colorado at Boulder, Boulder, U.S.A.
J.P. Cumalat, M.E. Dinardo, B.R. Drell, W.T. Ford, B. Heyburn, E. Luiggi Lopez, U. Nauenberg, K. Stenson, K. Ulmer, S.R. Wagner, S.L. Zang

Cornell University, Ithaca, U.S.A.
L. Agostino, J. Alexander, F. Blekman, D. Cassel, A. Chatterjee, S. Das, L.K. Gibbons, B. Heltsley, W. Hopkins, A. Khukhunaishvili, B. Kreis, V. Kuznetsov, J.R. Patterson, D. Puigh, A. Ryd, X. Shi, S. Stroiney, W. Sun, W.D. Teo, J. Thom, J. Vaughan, Y. Weng, P. Wittich

2010 JINST 5 T03016

Fairfield University, Fairfield, U.S.A.
C.P. Beetz, G. Cirino, C. Sanzeni, D. Winn

Fermi National Accelerator Laboratory, Batavia, U.S.A.
S. Abdullin, M.A. Afaq[1], M. Albrow, B. Ananthan, G. Apollinari, M. Atac, W. Badgett, L. Bagby, J.A. Bakken, B. Baldin, S. Banerjee, K. Banicz, L.A.T. Bauerdick, A. Beretvas, J. Berryhill, P.C. Bhat, K. Biery, M. Binkley, I. Bloch, F. Borcherding, A.M. Brett, K. Burkett, J.N. Butler, V. Chetluru, H.W.K. Cheung, F. Chlebana, I. Churin, S. Cihangir, M. Crawford, W. Dagenhart, M. Demarteau, G. Derylo, D. Dykstra, D.P. Eartly, J.E. Elias, V.D. Elvira, D. Evans, L. Feng, M. Fischler, I. Fisk, S. Foulkes, J. Freeman, P. Gartung, E. Gottschalk, T. Grassi, D. Green, Y. Guo, O. Gutsche, A. Hahn, J. Hanlon, R.M. Harris, B. Holzman, J. Howell, D. Hufnagel, E. James, H. Jensen, M. Johnson, C.D. Jones, U. Joshi, E. Juska, J. Kaiser, B. Klima, S. Kossiakov, K. Kousouris, S. Kwan, C.M. Lei, P. Limon, J.A. Lopez Perez, S. Los, L. Lueking, G. Lukhanin, S. Lusin[1], J. Lykken, K. Maeshima, J.M. Marraffino, D. Mason, P. McBride, T. Miao, K. Mishra, S. Moccia, R. Mommsen, S. Mrenna, A.S. Muhammad, C. Newman-Holmes, C. Noeding, V. O'Dell, O. Prokofyev, R. Rivera, C.H. Rivetta, A. Ronzhin, P. Rossman, S. Ryu, V. Sekhri, E. Sexton-Kennedy, I. Sfiligoi, S. Sharma, T.M. Shaw, D. Shpakov, E. Skup, R.P. Smith[†], A. Soha, W.J. Spalding, L. Spiegel, I. Suzuki, P. Tan, W. Tanenbaum, S. Tkaczyk[1], R. Trentadue[1], L. Uplegger, E.W. Vaandering, R. Vidal, J. Whitmore, E. Wicklund, W. Wu, J. Yarba, F. Yumiceva, J.C. Yun

University of Florida, Gainesville, U.S.A.
D. Acosta, P. Avery, V. Barashko, D. Bourilkov, M. Chen, G.P. Di Giovanni, D. Dobur, A. Drozdetskiy, R.D. Field, Y. Fu, I.K. Furic, J. Gartner, D. Holmes, B. Kim, S. Klimenko, J. Konigsberg, A. Korytov, K. Kotov, A. Kropivnitskaya, T. Kypreos, A. Madorsky, K. Matchev, G. Mitselmakher, Y. Pakhotin, J. Piedra Gomez, C. Prescott, V. Rapsevicius, R. Remington, M. Schmitt, B. Scurlock, D. Wang, J. Yelton

Florida International University, Miami, U.S.A.
C. Ceron, V. Gaultney, L. Kramer, L.M. Lebolo, S. Linn, P. Markowitz, G. Martinez, J.L. Rodriguez

Florida State University, Tallahassee, U.S.A.
T. Adams, A. Askew, H. Baer, M. Bertoldi, J. Chen, W.G.D. Dharmaratna, S.V. Gleyzer, J. Haas, S. Hagopian, V. Hagopian, M. Jenkins, K.F. Johnson, E. Prettner, H. Prosper, S. Sekmen

Florida Institute of Technology, Melbourne, U.S.A.
M.M. Baarmand, S. Guragain, M. Hohlmann, H. Kalakhety, H. Mermerkaya, R. Ralich, I. Vodopiyanov

University of Illinois at Chicago (UIC), Chicago, U.S.A.
B. Abelev, M.R. Adams, I.M. Anghel, L. Apanasevich, V.E. Bazterra, R.R. Betts, J. Callner, M.A. Castro, R. Cavanaugh, C. Dragoiu, E.J. Garcia-Solis, C.E. Gerber, D.J. Hofman, S. Khalatian, C. Mironov, E. Shabalina, A. Smoron, N. Varelas

The University of Iowa, Iowa City, U.S.A.
U. Akgun, E.A. Albayrak, A.S. Ayan, B. Bilki, R. Briggs, K. Cankocak[36], K. Chung, W. Clarida, P. Debbins, F. Duru, F.D. Ingram, C.K. Lae, E. McCliment, J.-P. Merlo, A. Mestvirishvili, M.J. Miller, A. Moeller, J. Nachtman, C.R. Newsom, E. Norbeck, J. Olson, Y. Onel, F. Ozok, J. Parsons, I. Schmidt, S. Sen, J. Wetzel, T. Yetkin, K. Yi

2010 JINST 5 T03016

Johns Hopkins University, Baltimore, U.S.A.
B.A. Barnett, B. Blumenfeld, A. Bonato, C.Y. Chien, D. Fehling, G. Giurgiu, A.V. Gritsan, Z.J. Guo, P. Maksimovic, S. Rappoccio, M. Swartz, N.V. Tran, Y. Zhang

The University of Kansas, Lawrence, U.S.A.
P. Baringer, A. Bean, O. Grachov, M. Murray, V. Radicci, S. Sanders, J.S. Wood, V. Zhukova

Kansas State University, Manhattan, U.S.A.
D. Bandurin, T. Bolton, K. Kaadze, A. Liu, Y. Maravin, D. Onoprienko, I. Svintradze, Z. Wan

Lawrence Livermore National Laboratory, Livermore, U.S.A.
J. Gronberg, J. Hollar, D. Lange, D. Wright

University of Maryland, College Park, U.S.A.
D. Baden, R. Bard, M. Boutemeur, S.C. Eno, D. Ferencek, N.J. Hadley, R.G. Kellogg, M. Kirn, S. Kunori, K. Rossato, P. Rumerio, F. Santanastasio, A. Skuja, J. Temple, M.B. Tonjes, S.C. Tonwar, T. Toole, E. Twedt

Massachusetts Institute of Technology, Cambridge, U.S.A.
B. Alver, G. Bauer, J. Bendavid, W. Busza, E. Butz, I.A. Cali, M. Chan, D. D'Enterria, P. Everaerts, G. Gomez Ceballos, K.A. Hahn, P. Harris, S. Jaditz, Y. Kim, M. Klute, Y.-J. Lee, W. Li, C. Loizides, T. Ma, M. Miller, S. Nahn, C. Paus, C. Roland, G. Roland, M. Rudolph, G. Stephans, K. Sumorok, K. Sung, S. Vaurynovich, E.A. Wenger, B. Wyslouch, S. Xie, Y. Yilmaz, A.S. Yoon

University of Minnesota, Minneapolis, U.S.A.
D. Bailleux, S.I. Cooper, P. Cushman, B. Dahmes, A. De Benedetti, A. Dolgopolov, P.R. Dudero, R. Egeland, G. Franzoni, J. Haupt, A. Inyakin[37], K. Klapoetke, Y. Kubota, J. Mans, N. Mirman, D. Petyt, V. Rekovic, R. Rusack, M. Schroeder, A. Singovsky, J. Zhang

University of Mississippi, University, U.S.A.
L.M. Cremaldi, R. Godang, R. Kroeger, L. Perera, R. Rahmat, D.A. Sanders, P. Sonnek, D. Summers

University of Nebraska-Lincoln, Lincoln, U.S.A.
K. Bloom, B. Bockelman, S. Bose, J. Butt, D.R. Claes, A. Dominguez, M. Eads, J. Keller, T. Kelly, I. Kravchenko, J. Lazo-Flores, C. Lundstedt, H. Malbouisson, S. Malik, G.R. Snow

State University of New York at Buffalo, Buffalo, U.S.A.
U. Baur, I. Iashvili, A. Kharchilava, A. Kumar, K. Smith, M. Strang

Northeastern University, Boston, U.S.A.
G. Alverson, E. Barberis, O. Boeriu, G. Eulisse, G. Govi, T. McCauley, Y. Musienko[38], S. Muzaffar, I. Osborne, T. Paul, S. Reucroft, J. Swain, L. Taylor, L. Tuura

Northwestern University, Evanston, U.S.A.
A. Anastassov, B. Gobbi, A. Kubik, R.A. Ofierzynski, A. Pozdnyakov, M. Schmitt, S. Stoynev, M. Velasco, S. Won

University of Notre Dame, Notre Dame, U.S.A.
L. Antonelli, D. Berry, M. Hildreth, C. Jessop, D.J. Karmgard, T. Kolberg, K. Lannon, S. Lynch, N. Marinelli, D.M. Morse, R. Ruchti, J. Slaunwhite, J. Warchol, M. Wayne

2010 JINST 5 T03016

The Ohio State University, Columbus, U.S.A.
B. Bylsma, L.S. Durkin, J. Gilmore[39], J. Gu, P. Killewald, T.Y. Ling, G. Williams

Princeton University, Princeton, U.S.A.
N. Adam, E. Berry, P. Elmer, A. Garmash, D. Gerbaudo, V. Halyo, A. Hunt, J. Jones, E. Laird, D. Marlow, T. Medvedeva, M. Mooney, J. Olsen, P. Piroué, D. Stickland, C. Tully, J.S. Werner, T. Wildish, Z. Xie, A. Zuranski

University of Puerto Rico, Mayaguez, U.S.A.
J.G. Acosta, M. Bonnett Del Alamo, X.T. Huang, A. Lopez, H. Mendez, S. Oliveros, J.E. Ramirez Vargas, N. Santacruz, A. Zatzerklyany

Purdue University, West Lafayette, U.S.A.
E. Alagoz, E. Antillon, V.E. Barnes, G. Bolla, D. Bortoletto, A. Everett, A.F. Garfinkel, Z. Gecse, L. Gutay, N. Ippolito, M. Jones, O. Koybasi, A.T. Laasanen, N. Leonardo, C. Liu, V. Maroussov, P. Merkel, D.H. Miller, N. Neumeister, A. Sedov, I. Shipsey, H.D. Yoo, Y. Zheng

Purdue University Calumet, Hammond, U.S.A.
P. Jindal, N. Parashar

Rice University, Houston, U.S.A.
V. Cuplov, K.M. Ecklund, F.J.M. Geurts, J.H. Liu, D. Maronde, M. Matveev, B.P. Padley, R. Redjimi, J. Roberts, L. Sabbatini, A. Tumanov

University of Rochester, Rochester, U.S.A.
B. Betchart, A. Bodek, H. Budd, Y.S. Chung, P. de Barbaro, R. Demina, H. Flacher, Y. Gotra, A. Harel, S. Korjenevski, D.C. Miner, D. Orbaker, G. Petrillo, D. Vishnevskiy, M. Zielinski

The Rockefeller University, New York, U.S.A.
A. Bhatti, L. Demortier, K. Goulianos, K. Hatakeyama, G. Lungu, C. Mesropian, M. Yan

Rutgers, the State University of New Jersey, Piscataway, U.S.A.
O. Atramentov, E. Bartz, Y. Gershtein, E. Halkiadakis, D. Hits, A. Lath, K. Rose, S. Schnetzer, S. Somalwar, R. Stone, S. Thomas, T.L. Watts

University of Tennessee, Knoxville, U.S.A.
G. Cerizza, M. Hollingsworth, S. Spanier, Z.C. Yang, A. York

Texas A&M University, College Station, U.S.A.
J. Asaadi, A. Aurisano, R. Eusebi, A. Golyash, A. Gurrola, T. Kamon, C.N. Nguyen, J. Pivarski, A. Safonov, S. Sengupta, D. Toback, M. Weinberger

Texas Tech University, Lubbock, U.S.A.
N. Akchurin, L. Berntzon, K. Gumus, C. Jeong, H. Kim, S.W. Lee, S. Popescu, Y. Roh, A. Sill, I. Volobouev, E. Washington, R. Wigmans, E. Yazgan

Vanderbilt University, Nashville, U.S.A.
D. Engh, C. Florez, W. Johns, S. Pathak, P. Sheldon

University of Virginia, Charlottesville, U.S.A.
D. Andelin, M.W. Arenton, M. Balazs, S. Boutle, M. Buehler, S. Conetti, B. Cox, R. Hirosky, A. Ledovskoy, C. Neu, D. Phillips II, M. Ronquest, R. Yohay

2010 JINST 5 T03016

Wayne State University, Detroit, U.S.A.
S. Gollapinni, K. Gunthoti, R. Harr, P.E. Karchin, M. Mattson, A. Sakharov

University of Wisconsin, Madison, U.S.A.
M. Anderson, M. Bachtis, J.N. Bellinger, D. Carlsmith, I. Crotty[1], S. Dasu, S. Dutta, J. Efron, F. Feyzi, K. Flood, L. Gray, K.S. Grogg, M. Grothe, R. Hall-Wilton[1], M. Jaworski, P. Klabbers, J. Klukas, A. Lanaro, C. Lazaridis, J. Leonard, R. Loveless, M. Magrans de Abril, A. Mohapatra, G. Ott, G. Polese, D. Reeder, A. Savin, W.H. Smith, A. Sourkov[40], J. Swanson, M. Weinberg, D. Wenman, M. Wensveen, A. White

†: Deceased
1: Also at CERN, European Organization for Nuclear Research, Geneva, Switzerland
2: Also at Universidade Federal do ABC, Santo Andre, Brazil
3: Also at Soltan Institute for Nuclear Studies, Warsaw, Poland
4: Also at Université de Haute-Alsace, Mulhouse, France
5: Also at Centre de Calcul de l'Institut National de Physique Nucleaire et de Physique des Particules (IN2P3), Villeurbanne, France
6: Also at Moscow State University, Moscow, Russia
7: Also at Institute of Nuclear Research ATOMKI, Debrecen, Hungary
8: Also at University of California, San Diego, La Jolla, U.S.A.
9: Also at Tata Institute of Fundamental Research - HECR, Mumbai, India
10: Also at University of Visva-Bharati, Santiniketan, India
11: Also at Facolta' Ingegneria Universita' di Roma "La Sapienza", Roma, Italy
12: Also at Università della Basilicata, Potenza, Italy
13: Also at Laboratori Nazionali di Legnaro dell' INFN, Legnaro, Italy
14: Also at Università di Trento, Trento, Italy
15: Also at ENEA - Casaccia Research Center, S. Maria di Galeria, Italy
16: Also at Warsaw University of Technology, Institute of Electronic Systems, Warsaw, Poland
17: Also at California Institute of Technology, Pasadena, U.S.A.
18: Also at Faculty of Physics of University of Belgrade, Belgrade, Serbia
19: Also at Laboratoire Leprince-Ringuet, Ecole Polytechnique, IN2P3-CNRS, Palaiseau, France
20: Also at Alstom Contracting, Geneve, Switzerland
21: Also at Scuola Normale e Sezione dell' INFN, Pisa, Italy
22: Also at University of Athens, Athens, Greece
23: Also at The University of Kansas, Lawrence, U.S.A.
24: Also at Institute for Theoretical and Experimental Physics, Moscow, Russia
25: Also at Paul Scherrer Institut, Villigen, Switzerland
26: Also at Vinca Institute of Nuclear Sciences, Belgrade, Serbia
27: Also at University of Wisconsin, Madison, U.S.A.
28: Also at Mersin University, Mersin, Turkey
29: Also at Izmir Institute of Technology, Izmir, Turkey
30: Also at Kafkas University, Kars, Turkey
31: Also at Suleyman Demirel University, Isparta, Turkey
32: Also at Ege University, Izmir, Turkey

2010 JINST 5 T03016

33: Also at Rutherford Appleton Laboratory, Didcot, United Kingdom
34: Also at INFN Sezione di Perugia; Universita di Perugia, Perugia, Italy
35: Also at KFKI Research Institute for Particle and Nuclear Physics, Budapest, Hungary
36: Also at Istanbul Technical University, Istanbul, Turkey
37: Also at University of Minnesota, Minneapolis, U.S.A.
38: Also at Institute for Nuclear Research, Moscow, Russia
39: Also at Texas A&M University, College Station, U.S.A.
40: Also at State Research Center of Russian Federation, Institute for High Energy Physics, Protvino, Russia

2010 JINST 5 T03016